

AFRL-VA-WP-TR-1999-3030

**UPDATE OF THE PROBABILITY OF
FRACTURE (PROF) COMPUTER
PROGRAM FOR AGING AIRCRAFT
RISK ANALYSIS**



Volume 1 Modifications and User's Guide

Peter W. Hovey
Air Force Research Laboratory
AFRL/VASE
WPAFB OH 45433-7402

Alan P. Berens and John S. Loomis
University of Dayton Research Institute
1300 Shroyer Park Center
Dayton, OH 45469-0120

NOVEMBER 1998

FINAL REPORT FOR PERIOD SEPTEMBER 1996 – NOVEMBER 1998

Approved for public release; distribution unlimited

**AIR VEHICLES DIRECTORATE
AIR FORCE RESEARCH LABORATORY
AIR FORCE MATERIEL COMMAND
WRIGHT-PATTERSON AIR FORCE BASE, OH 45433-7542**

19990513 108


DTIC QUALITY INSPECTED 4

NOTICE

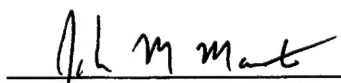
USING GOVERNMENT DRAWINGS, SPECIFICATIONS, OR OTHER DATA INCLUDED IN THIS DOCUMENT FOR ANY PURPOSE OTHER THAN GOVERNMENT PROCUREMENT DOES NOT IN ANY WAY OBLIGATE THE US GOVERNMENT. THE FACT THAT THE GOVERNMENT FORMULATED OR SUPPLIED THE DRAWINGS, SPECIFICATIONS, OR OTHER DATA DOES NOT LICENSE THE HOLDER OR ANY OTHER PERSON OR CORPORATION; OR CONVEY ANY RIGHTS OR PERMISSION TO MANUFACTURE, USE , OR SELL ANY PATENTED INVENTION THAT MAY RELATE TO THEM.

THIS REPORT IS RELEASABLE TO THE NATIONAL TECHNICAL INFORMATION SERVICE (NTIS). AT NTIS, IT WILL BE AVAILABLE TO THE GENERAL PUBLIC, INCLUDING FOREIGN NATIONS.

THIS TECHNICAL REPORT HAS BEEN REVIEWED AND IS APPROVED FOR PUBLICATION.

 FOR
MAJ. SCOTT A. FAWAZ
PROJECT MONITOR
STRUCTURAL INTEGRITY BRANCH


JOHN T. ACH
CHIEF
STRUCTURAL INTEGRITY BRANCH


JOSEPH M. MANTER
CHIEF
STRUCTURES DIVISION

Do not return copies of this report unless contractual obligations or notice on a specific document requires its return.

| REPORT DOCUMENTATION PAGE | | | Form Approved OMB No. 0704-0188 | |
|---|---|--|---|--|
| Public reporting burden for this collection of information is estimated to average 1 hour per response, including the time for reviewing instructions, searching existing data sources, gathering and maintaining the data needed, and completing and reviewing the collection of information. Send comments regarding this burden estimate or any other aspect of this collection of information, including suggestions for reducing this burden, to Washington Headquarters Services, Directorate for Information Operations and Reports, 1215 Jefferson Davis Highway, Suite 1204, Arlington, VA 22202-4302, and to the Office of Management and Budget, Paperwork Reduction Project (0704-0188), Washington, DC 20503. | | | | |
| 1. AGENCY USE ONLY (Leave blank) | | 2. REPORT DATE November 1998 | 3. REPORT TYPE AND DATES COVERED FINAL REPORT- SEP 96 - NOV 98 | |
| 4. TITLE AND SUBTITLE Update Of The Probability Of Fracture (Prof) Computer Program For Aging Aircraft Risk Analysis Volume 1 Modifications And User's Guide | | | 5. FUNDING NUMBERS C: F09603-95-D-0175 PE: JMF090 PR: FAAF TA: 92 WU: 00 | |
| 6. AUTHOR(S) Peter W. Hovey, AFRL/VASE Alan P. Berens and John S. Loomis, UDRI | | | | |
| 7. PERFORMING ORGANIZATION NAME(S) AND ADDRESS(ES) Air Force Research Laboratory, AFRL/VASE, 2790 D St. RM 504, WPAFB, OH 45433-7402 University of Dayton Research Institute, Room 1300 Shroyer Park Center, Dayton OH 45469-0120 | | | 8. PERFORMING ORGANIZATION REPORT NUMBER UDR-TR-1998-00154 | |
| 9. SPONSORING/MONITORING AGENCY NAME(S) AND ADDRESS(ES) Air Vehicles Directorate Air Force Research Laboratory Air Force Materiel Command Wright-Patterson Air Force Base, Oh 45433-7562 POC: Maj Scott A Fawaz, AFRL/VASE, 937-255-6104 x239 | | | 10. SPONSORING/MONITORING AGENCY REPORT NUMBER AFRL-VA-WP-TR-1999-3030 | |
| 11. SUPPLEMENTARY NOTES This material may be reproduced by or for the U.S. Government pursuant to the copyright license under the clause at DFARS 252.227-7013 Oct 88. | | | | |
| 12a. DISTRIBUTION AVAILABILITY STATEMENT APPROVED FOR PUBLIC RELEASE; DISTRIBUTION UNLIMITED | | | 12b. DISTRIBUTION CODE | |
| 13. ABSTRACT (Maximum 200 words) The computer program, PRObability Of Fracture (PROF) was written to facilitate the Air Force implementation of structural risk analyses. The fracture probabilities from a PROF run directly complement the deterministic damage tolerance analyses that form the bases for structural maintenance actions. However, there are many structural scenarios that cannot be modeled directly by a single PROF run, but can be analyzed through the combination of multiple PROF runs. These include the scenarios introduced by widespread fatigue damage and corrosive thinning. While these more complex applications of PROF have been demonstrated, they were difficult to implement because of the post processing required of the individual PROF runs. Further, to accommodate the calculation of failure due to discrete source damage in the presence of widespread fatigue damage, a different failure criterion was needed. Therefore, PROF was updated to accommodate these calculations and to incorporate more robust computational algorithms. This report describes the modifications made to PROF and serves as a users guide for the program. Volume 2 is a programmers guide to the PROF software. | | | | |
| 14. SUBJECT TERMS Aging Aircraft, Probabilistic Risk Assessment, Probabilistic Fracture Mechanics, Fleet Management | | | 15. NUMBER OF PAGES 96 | |
| | | | 16. PRICE CODE | |
| 17. SECURITY CLASSIFICATION OF REPORT Unclassified | 18. SECURITY CLASSIFICATION OF THIS PAGE Unclassified | 19. SECURITY CLASSIFICATION OF ABSTRACT Unclassified | 20. LIMITATION OF ABSTRACT SAR | |

Table of Contents

| | |
|--|-----|
| List of Figures | v |
| List of Tables | vii |
| Foreword | ix |
| Section 1 Introduction | 1 |
| 1.1 Background | 1 |
| 1.2 Problem Statement/Objectives | 2 |
| 1.2.1 Discrete Source Damage | 3 |
| 1.2.2 Facilitating Model Complexity | 4 |
| 1.2.3 Update of PROF Computations | 5 |
| Section 2 Previous Versions of PROF | 7 |
| Section 3 Analysis of Discrete Source Damage | 11 |
| 3.1 General Problem Statement | 11 |
| 3.2 Details of the Approach | 13 |
| 3.3 Example | 16 |
| Section 4 Multi-Run Data Management | 21 |
| 4.1 General Analysis Framework | 21 |
| 4.2 Lap Joint MSD/Corrosion Example | 23 |
| 4.2.1 MSD/Corrosion Example PROF Input | 27 |
| 4.2.2 MSD/Corrosion Example PROF Results | 29 |
| 4.2.3 MSD/Corrosion Example Summary | 35 |
| 4.3 Multi-Element Damage Example | 35 |
| 4.3.1 WS405 Problem Statement | 36 |
| 4.3.2 Selected WS405 Risk Analysis Results | 39 |
| 4.3.3 Multi-Element Damage Example Summary | 42 |
| Section 5 Additional Modifications to PROF | 43 |
| 5.1 User Interface | 43 |
| 5.2 Excel Interface | 45 |
| 5.3 Probability of Fracture | 46 |
| 5.4 Residual Strength Function Input | 47 |
| 5.5 Multi-Run Data Management | 47 |
| Section 6 Summary and Recommendations | 49 |
| Section 7 References | 51 |
| Appendix A PROF Users Manual | A-1 |
| A.1 PROF Installation | A-1 |
| A.2 Starting PROF | A-1 |
| A.3 PROF File Operations | A-2 |
| A.3.1 Opening a New Input File | A-2 |
| A.3.2 Opening Existing Input Files | A-2 |
| A.3.3 Save and Save As Menu Items | A-3 |
| A.3.4 Import Menu Item | A-3 |
| A.3.5 Exiting PROF | A-4 |
| A.4 Modifying the Input Sheet | A-4 |

Table of Contents (Cont'd.)

| | | |
|------------|--|------|
| | A.5 Data | A-5 |
| | A.5.1 Files | A-5 |
| | A.5.2 System Properties | A-5 |
| | A.6 Selecting a Case | A-6 |
| | A.7 Analysis | A-7 |
| | A.7.1 Standard Analysis Options | A-7 |
| | A.7.2 Residual Strength Analysis | A-10 |
| | A.8 Detail Calculations | A-11 |
| | A.8.1 Elapsed Time | A-12 |
| | A.8.2 Time Interval | A-14 |
| | A.8.3 Inspection | A-16 |
| | A.9 Viewing Data Files | A-18 |
| Appendix B | Numerical Methods in PROF | B-1 |
| | B.1 Probability of Fracture | B-1 |
| | B.2 Calculating Probability of Failure versus Crack Size | B-3 |
| | B.3 Probability of Failure During Flight | B-4 |
| | B.4 Verification of Calculations | B-5 |
| | B.4.1 Example 1 | B-5 |
| | B.4.2 Example 2 | B-7 |
| | B.4.3 Example 3 | B-9 |
| | B.5 Inspection and Repair Calculations | B-10 |
| | B.6 Procedure for Inspection and Repair Calculations | B-11 |

List of Figures

| | | |
|-----------|--|----|
| Figure 1 | Schematic of PROF..... | 7 |
| Figure 2 | Schematic of Projection of Crack Size Distribution | 8 |
| Figure 3 | Illustration of Residual Strength Calculation from Swift..... | 13 |
| Figure 4 | Plot of the Joint Probability Density Function of Crack Length and Peak Stress.... | 15 |
| Figure 5 | Schematic of the B-707 Wing and Side View of the Skin and Stringer Structure... | 16 |
| Figure 6 | Crack Growth Curve for Stringer 7 with All Structure Intact..... | 17 |
| Figure 7 | Peak Stress Distribution with DSD Present | 18 |
| Figure 8 | Residual Strength as a Function of Crack Length in Stringer 7..... | 18 |
| Figure 9 | Comparison of the Flaw Size Density Function at 40,000 Hours with the Density Function at 57,382 Hours..... | 19 |
| Figure 10 | Comparison of Single-Flight Probability of Failure Starting from 57,382 Hours versus 40,000 Hours..... | 20 |
| Figure 11 | Schematic of Lap Joint Specimen | 24 |
| Figure 12 | Conditional Failure Probabilities for 2 MSD Scenarios and 5 Levels of Uniform Thickness Loss | 26 |
| Figure 13 | Crack Size versus Cycles for Scenario 1..... | 28 |
| Figure 14 | Crack Size versus Cycles for Scenario 2..... | 28 |
| Figure 15 | Weibull Mixture of Initial Crack Sizes | 29 |
| Figure 16 | POF versus Cycles for Scenario 1..... | 30 |
| Figure 17 | POF versus Cycles for Scenario 2..... | 30 |
| Figure 18 | POF versus Cycles for Scenarios 1 and 2 Showing Comparison with Observed Data | 31 |
| Figure 19 | POF versus Cycles for Composite of Scenarios 1 and 2 Showing Comparison with Observed Data..... | 32 |
| Figure 20 | POF versus Cycles for Scenario Composites..... | 32 |
| Figure 21 | Example Histogram of Levels of Corrosion Damage – Severity Mix 3 | 33 |
| Figure 22 | Example Histogram of Cycles to POF = 0.0001 – Severity Mix 3..... | 33 |
| Figure 23 | Cumulative Distribution of Cycles to Selected POF – 3 Corrosion Severities | 34 |
| Figure 24 | Risk Ratios Normalized to No Corrosion Condition | 34 |
| Figure 25 | WS405 Fault Tree | 37 |
| Figure 26 | WS405 Venn Diagram | 38 |
| Figure 27 | Failure Probabilities of Splice Fitting and Beam Cap..... | 40 |
| Figure 28 | Conditional Failure Probabilities of Chordwise Joint | 41 |
| Figure 29 | Unconditional Probability of Failure of Chordwise Joint | 41 |
| Figure 30 | Unconditional Probability of Failure of Chordwise Joint – With and Without Initial Inspection/Repair..... | 42 |
| Figure 31 | Screen Layout for New Version of PROF | 44 |
| Figure 32 | Example of a PROF Input Worksheet..... | 45 |
| Figure 33 | Example of a Multi-Run Input Worksheet..... | 47 |
| Figure 34 | Example of a Multi-Run Output Worksheet | 48 |

List of Figures (Cont'd.)

| | | |
|-------------|---|------|
| Figure A-1 | PROF File Menu | A-2 |
| Figure A-2 | Example of PROF Input Worksheet..... | A-3 |
| Figure A-3 | PROF Data Menu | A-5 |
| Figure A-4 | PROF Data - System Properties Menu..... | A-6 |
| Figure A-5 | PROF Case Menu | A-6 |
| Figure A-6 | Prof Case - Select Menu..... | A-7 |
| Figure A-7 | PROF Analysis Menu..... | A-7 |
| Figure A-8 | Example Screen After a Single-Case Analysis | A-8 |
| Figure A-9 | Example Worksheet for a Single-Case Analysis..... | A-9 |
| Figure A-10 | Example of Results Worksheet..... | A-10 |
| Figure A-11 | Example Display for POF(a)..... | A-11 |
| Figure A-12 | PROF Detail Menu | A-11 |
| Figure A-13 | PROF Detail-Time Since Inspection Menu..... | A-12 |
| Figure A-14 | Example Elapsed Time Calculation Screen..... | A-12 |
| Figure A-15 | Example of Detail - Elapsed Time Spreadsheet..... | A-14 |
| Figure A-16 | PROF Detail - Time Interval Menu..... | A-14 |
| Figure A-17 | Example Time Interval Calculation Screen | A-15 |
| Figure A-18 | Example Worksheet Created by Selecting Detail -Time-Interval | A-15 |
| Figure A-19 | PROF Detail - Inspection Menu | A-16 |
| Figure A-20 | Example Inspection Calculation Screen | A-16 |
| Figure A-21 | Example of Spreadsheet Generated by the Detail - Inspection Menu Item | A-17 |
| Figure A-22 | PROF View Menu..... | A-18 |
| Figure A-23 | PROF Screen Buttons..... | A-18 |
| Figure A-24 | Sample View Output for Different Data Files | A-19 |

List of Tables

| | | |
|-----------|---|-----|
| Table B-1 | Example 1: Details of the Calculation of the Probability of Failure..... | B-6 |
| Table B-2 | Example 1: Summary of Results..... | B-6 |
| Table B-3 | Example 1: Comparison of Failure Probabilities for Crack Size Distribution Extrapolation..... | B-7 |
| Table B-4 | Example 2: Summary of Results..... | B-7 |
| Table B-5 | Example 2: Details of the Calculation of the Probability of Failure..... | B-8 |
| Table B-6 | Example 2: Comparison of Failure Probabilities for Crack Size Distribution in Extrapolations | B-8 |
| Table B-7 | Example 3: Summary of Results..... | B-9 |

Foreword

This technical report was prepared by the Structural Integrity Division of the University of Dayton Research Institute for the Air Vehicles Directorate of the Air Force Research Laboratory, Wright-Patterson Air Force Base, Ohio. The work was performed under Contract Number F09603-95-D-0175 (Order No. RZ03) with Major Scott Fawaz (WL/VASE) as the Air Force project monitor. The work was performed between September 1996 and November 1998 with Dr. Alan P. Berens of the University of Dayton Research Institute as the Principal Investigator.

The final report of this work comprises two volumes. Volume 1 contains a description of the changes made in updating the Probability Of Fracture Code (PROF), representative examples of the added capability and a User's Manual. Volume 2 contains a programmer guide to the PROF software.

Section 1

Introduction

Structural risk analysis is an additional fleet management tool that is increasingly being used for decisions regarding the timing and extent of inspection, repair, or replacement maintenance actions on critical structural details. Structural risk analysis is based on the probability of failure in a defined population of structurally significant details. In a fatigue environment, this probabilistic evaluation of strength versus stress is dynamic, since strength degrades as fatigue cracks initiate and grow. Fracture mechanics provides deterministic tools that predict the growth of cracks for fixed stress sequences from an initial size to critical size. By introducing probabilistic descriptions of the factors that produce different initiating conditions and crack growth in the population, the results from deterministic tools can be extended to quantify the degree of safety during an operating period.

The computer program, PRobability Of Fracture (PROF) was written to facilitate the Air Force implementation of structural risk analyses. The fracture probabilities from a PROF run directly complement the deterministic damage tolerance analyses that form the bases for structural maintenance actions. However, there are many structural scenarios that cannot be modeled directly by a single PROF run, but can be analyzed through the combination of multiple PROF runs. These include the scenarios introduced by widespread fatigue damage and corrosive thinning. While these more complex applications of PROF have been demonstrated, they were difficult to implement because of the post processing required of the individual PROF runs. Further, to accommodate the calculation of failure due to discrete source damage in the presence of widespread fatigue damage, a different failure criterion was needed. Therefore, PROF was updated to accommodate these calculations and to incorporate more robust computational algorithms. Descriptions of the modifications made to PROF are the subject of this report.

1.1 Background

The Air Force ensures structural integrity through inspections based on a deterministic analysis of the growth of potential monolithic cracks that are assumed to be present in each critical location in an airframe. This approach has been successful to date but, on several occasions, struc-

tural risk analyses were employed to better assess the potential for failures associated with the stochastic elements of fatigue cracking [1, 2, 3]. These supplemental analyses impacted decisions concerning maintenance (inspection) intervals and the timing of modification actions. Accordingly, the Air Force developed the structural risk analysis computer program Probability Of Fracture (PROF), called WinPROF in the Windows version, as a tool to be used by the Air Logistics Centers in making decisions related to the timing of maintenance actions in the aging aircraft fleets.

Failure risks associated with the initiation and growth of fatigue cracks are governed by the crack sizes, the loads experienced by the aircraft, the geometry of the structure at the damage sites, the scatter in the material properties, and the inspection frequency and capability. Because of the stochastic nature of these factors, their joint effects are best described in terms of a probabilistic model. All of these factors have been incorporated in the PROF computer code, but this code is directed primarily at cracking scenarios dominated by a single crack. The basic PROF run produces failure probabilities for a single structural geometry based on the Irwin fracture criterion. The output of a PROF run comprises a summary of the input conditions, failure probability as a function of time, and the distribution of the crack sizes before and after an inspection. In the original versions of the program, the output from each run was stored in text (ASCII) files.

As a fleet ages, however, the need for more complex damage scenarios becomes apparent. The potential for widespread fatigue damage (WFD) increases significantly and structural safety can no longer be evaluated in terms of a single monolithic crack from a critical location. The interacting effects of changing stresses and stress intensity factors must be taken into account. Further, the possible presence of cracking in adjacent structure can affect fail safety so that the failure probability associated with discrete source damage must also be evaluated.

1.2 Problem Statement/Objectives

PROF was originally developed to perform probabilistic risk analyses related to the primary failure mode of fatigue crack growth in a metallic aging aircraft structure. Since the initial development of PROF, other damage scenarios associated with aging aircraft have been identified and investigated. The newly-identified risk analysis scenarios include: a) discrete source damage in the presence of MSD; b) WFD (both multi-site damage and multi-element damage); and, c) the

potential effect of corrosive thinning in a fleet. The primary goals of this contract were to develop appropriate tools within the PROF analysis system to facilitate probabilistic risk analysis of these damage scenarios. Two additional capabilities were added to PROF to accomplish these goals: probabilistic risk assessment of discrete source damage and a multi-run data management capability. A secondary, but necessary, goal was to modernize the Windows user interface and improve the calculation algorithms of the original PROF code. The following subsections provide a general description of the changes to the PROF system. Detailed discussions of these changes comprise the major sections of the report.

1.2.1 Discrete Source Damage

The discrete source damage (DSD) problem refers to the ability of a structural component to perform its fail-safe function in the event that an adjacent structural member fails. The failure of the structural member could be caused, for example, by discrete events such as battle damage and uncontained engine disk failure, or by fatigue crack growth. The presence of multi-site damage (MSD) could degrade the ability of a structural component to carry the additional load when discrete source damage occurs. Much of the research into the effects of multi-site damage has been concerned with the conditions under which many small cracks would link into one large crack. However, the degradation of the fail-safe capability would occur long before link-up conditions were present.

The main emphasis in the discrete source damage problem is the conditional probability of failure of the fail-safe structure, given that the discrete source damage has occurred. Prior to the discrete source damage, the flaw size distribution changes in time exactly as in a standard PROF run, since all structure are intact. However, the fracture criterion is different after the discrete source damage is incurred. The shifting of load due to the loss of a structural element can be complex and may not be modeled by the Irwin abrupt fracture criteria. A change in the fracture criteria was required to analyze discrete source damage.

A typical structural analysis of a fail-safe structure in the presence of discrete source damage produces the residual strength as a function of crack size. The residual strength calculation includes the effects of the complex stress fields caused by the discrete source damage, as

well as the fracture toughness of the material. This characterization of residual strength results in a simpler calculation than a standard PROF analysis, since fracture toughness is not included as a random variable. The discrete source damage objective was met by adding a new algorithm to PROF to calculate the conditional probability of failure, given that an adjacent structural element is in a failed state. Details of this analysis are discussed in Section 3.

1.2.2 Facilitating Model Complexity

A single run of PROF produces the probability of failure as a function of flight hours for the specific set of fracture mechanics conditions that governed the input to the run. These fracture mechanics conditions determine the population to which the probability applies. There are many applications that require distinct analyses for different or changing structural conditions. When the relative frequency of occurrence for the different sets of conditions is known in a larger population of interest, the PROF-generated conditional probabilities can be combined to provide overall unconditional failure probabilities for the larger population. For example, in multi-element damage problems, the failure of one element does not lead to failure of the structure, but can impact the stresses on an adjacent element, which could lead to failure of the structure. Each sub-population (combination of failed and intact adjacent elements) must be analyzed with a separate PROF run. The conditional failure probabilities would then be combined to calculate the unconditional probability of fracture for the multi-element structure.

These more complex scenarios can be analyzed using the original PROF, but considerable effort is required to perform the necessary post-processing of the ASCII output files. Since risk analyses for a large number of essentially different damage scenarios can be anticipated, the objective of facilitating the analyses of MSD and corrosion scenarios was met by incorporating an Excel Workbook interface for a multi-run data management capability. The updated PROF can perform multiple runs in one analysis and stores the PROF results on pages of an Excel Workbook. The analyst has available all of the macro and plotting capability of Excel and can easily combine the conditional failure probabilities in accordance with the specific damage scenario being analyzed. The approach to analyzing different damage scenarios and an MSD/corrosion example are presented in Section 4.

1.2.3 Update of PROF Computations

The original PROF code was written about 1990. A third-party user interface was later used to add a graphical, Windows front end for application on a personal computer. Since relatively major changes to the program were to be incorporated for the new capability, the entire program was modernized. In particular, a Microsoft application program was substituted for the third-party user interface, allowing the use of Windows common dialog boxes. Further, the FORTRAN code for performing the calculations was converted to C++.

The computational algorithms of the original PROF occasionally produced anomalous results that were primarily attributed to the integration methodology applied to the tails of the input distributions. For example, the original PROF computational algorithm continually updated the flaw size distribution table for each calculation of a single flight probability of failure. This approach ran quickly, but it also led to the program failing when the crack size distribution got too large and to inconsistencies in the calculation of failure probability because of the approach for handling the tail of the crack size distribution functions. New algorithms that perform a more direct calculation have been incorporated in the updated PROF. The tails of these distribution functions were stabilized by converting crack lengths to "ages" through the deterministic crack growth function. "Growing" the age distribution is a simple linear shift so that the tail remains stable. The age distribution is affected by the shape of the crack growth curve and, in specific problems, it was noted that the probability of fracture at time zero was affected by the crack growth curve.

Since the original development of PROF, computing speed has increased dramatically. Problems that took up to 30 minutes when PROF was first converted to the PC now take seconds. It is now reasonable to use longer algorithms that are intrinsically more stable. The flaw size distribution table is no longer updated for each time step. The integral for each time step is performed over the flaw size distribution at time zero. The crack growth curve is used to project the crack size to the current time step to determine the residual strength for each call of the integrand in the numerical quadrature. Complete details of the new algorithms are contained in Section 5 and Appendix B.

Section 2

Previous Versions of PROF

PROF is a fracture-based risk analysis program for calculating the increasing probabilities of failure associated with the growing fatigue cracks in metallic structure [4]. The original version of PROF was written in FORTRAN and was executed on a VAX 11-780 minicomputer under the VMS operating system [5]. PROF was later converted to run in the Windows environment on a personal computer and this PC version is referred to as WinPROF [6].

PROF was specifically written to interface with the data that is available as a result of ASIP, Figure 1. Under ASIP, crack life predictions (a versus T) are available for every known critical location. This implies the availability of: a) the flight-by-flight stress spectrum, from which the distribution of maximum stress per flight can be obtained; b) stress intensity factors as a function of crack size, a versus K/σ , and c) fracture toughness, K_{cr} , from which a distribution of fracture toughness can be inferred. The initiating crack size distribution can be obtained from inspection feedback, tear-down inspections, or equivalent initial flaw sizes. Probability of detection as a function of crack size, $POD(a)$, is a characterization of the capability of the non-destructive inspection system used during the safety inspections.

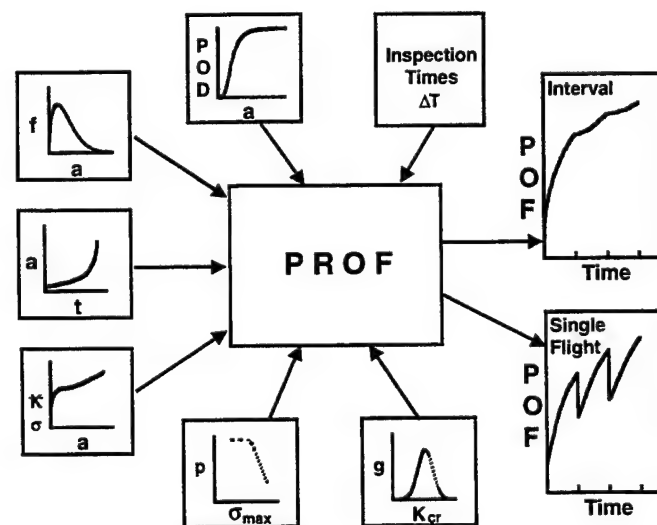


Figure 1. Schematic of PROF

The starting point of a PROF analysis (time zero) is the fleet flight hour age represented by the initiating crack size distribution. PROF uses the deterministic a versus T curve to project the percentiles of the initiating crack size distribution as a function of flight hours, Figure 2. At defined flight hour increments, the single-flight probability of fracture is calculated from the distributions of crack size, maximum stress per flight, and fracture toughness. That is, the single-flight fracture probability is the probability that the maximum stress intensity factor (combination of the distributions of maximum stress per flight and crack sizes) during the flight exceeds the critical stress intensity factor.

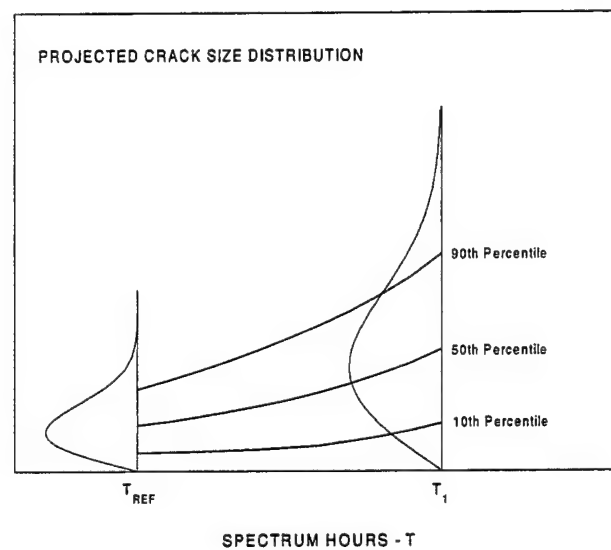


Figure 2. Schematic of Projection of Crack Size Distribution

At a maintenance cycle, the distribution of crack sizes is changed in accordance with the $POD(a)$ function and the equivalent repair crack size distribution. It is assumed that all detected cracks are repaired and the equivalent repair crack size distribution accounts for the repaired cracks. PROF produces files of both the pre- and post- inspection crack size distributions. The availability of these distributions allows changing the analysis conditions at inspection times set by the analyst.

The a versus T , a versus K/σ , and crack size distributions are input to PROF in tabular form. Fracture toughness is modeled by a normal distribution and requires values for the mean and standard deviation. Maximum stress per flight is modeled by the Gumbel extreme value distribution and the parameters of the distribution can be obtained from a fit of either a flight-by-

flight stress spectrum or an exceedance curve of all of the stresses in the spectrum. The $POD(a)$ function is modeled by a cumulative lognormal distribution with parameters μ and σ . Fifty percent of the cracks of size μ would be detected. The parameter, σ , determines the flatness of the $POD(a)$ function with smaller values implying steeper $POD(a)$ functions.

Sensitivity studies have been performed on the application of PROF in representative problems [4]. These studies have indicated that, although the absolute magnitudes of the fracture probabilities are strongly dependent on the input, relative magnitudes tend to remain consistent when factors are varied one at a time. Because of the indefinite nature of some of the input data, particularly the crack size information, absolute magnitudes of the fracture probabilities are suspect. However, it is believed that relative differences resulting from consistent variations in the better-defined input factors are meaningful.

A single run of PROF analyzes the growth of a crack for a single geometry, including crack type and shape. The inspection intervals are set by the analyst, including the possibility for an immediate inspection at time zero. The analysis would apply to the population of structural details that both have this geometry and are subject to an equivalent stress spectrum. The output summary file includes a record of the input file names and parameters, as well as the resulting fracture probabilities for a single structural detail, for a single aircraft when there are multiple equivalent details, and for the entire fleet. The distributions of the crack sizes before and after each inspection are also available.

In the original PROF and WinPROF, the output from each run was written to an ASCII file. More complex problems have been analyzed either by using intermediate crack size distributions from a previous PROF run or by combining the results from multiple runs. In the original PROF, such analyses first require importing the ASCII output files into a spreadsheet and then performing the required data processing. This required post-processing is cumbersome.

Section 3

Analysis of Discrete Source Damage

One goal of the Damage Tolerant Design (DTD) concept is to minimize the possibility of catastrophic failure when a partial structural failure occurs. The tools used to achieve this goal include crack-stopping structures and redundant load paths. If a partial failure occurs in a damage-tolerant structure, neighboring structural elements should be able to sustain the additional load through the conclusion of the current mission. The partial structural failure is sometimes referred to as Discrete Source Damage (DSD) because anticipated causes of the damage include discrete events such as battle damage or an uncontained engine failure.

Various studies have shown a detrimental effect on damage tolerance in the presence of widespread fatigue damage (WFD). Swift [7] provides definitions of concepts associated with WFD and illustrations of residual strength calculations for MSD. The Industry Committee on WFD published a report [8] that describes susceptible structures and provides guidelines for analyzing the effects of WFD. Both of these references point to the loss of residual strength in the presence of DSD as a critical concern when multi-site damage is present.

This section discusses the DSD problem and the analysis capability that has been added to PROF to evaluate the impact of MSD in the presence of partial damage. The first subsection provides a general description of the objectives for the PROF capability, the second subsection describes the analysis approach, and the last subsection describes an example problem.

3.1 General Problem Statement

Evaluating the impact of the loss of residual strength due to MSD poses an interesting challenge. Any loss of strength would usually result in the component not meeting design specifications with regard to limit load. However, the design specifications are very conservative so that the high load associated with the design is not likely to occur. The goal of DTD is to land the plane safely in the event of a partial structural failure. A probabilistic risk assessment can provide the single flight probability of failure for a damage-tolerant structure in the presence of DSD.

Lincoln [9] proposes the following definition for the onset of WFD: "The onset of wide-spread fatigue cracking is that point in the operational life of an aircraft when the damage tolerance or fail-safe capability of a structure has been degraded such that, after partial structural failure, the probability of failure of the structure does not meet the thresholds specified by the procuring (or certification) agency." The probability-based definition combines an engineering analysis of the residual strength with the random nature of accumulated damage and load environment to provide an evaluation of the likelihood that damage tolerant structure will not fail in the event of partial structural failure.

In keeping with this definition, an appropriate measure of the severity of WFD in a structural element is the conditional probability of failure, given that discrete source damage has occurred in a neighboring structural element. This conditional probability should be calculated as a function of time in service to determine the onset of WFD. The goal of the DSD module in the PROF system is to estimate the conditional probability of failure, given that DSD has occurred, based on the same assumptions used in the basic PROF calculation for generalized cracking.

The assumptions for the DSD module include the availability of the basic ASIP data for the structure, i.e., an anticipated load spectrum, a fracture mechanics analysis, and a crack growth curve under the anticipated usage. Also, it is assumed that there is some information about the current crack size distribution and the probability of detection function and repair quality if inspection intervals are included in the analysis. In addition to the usual data requirements for a standard PROF analysis, the DSD analysis requires an evaluation of the residual strength in the presence of partial structural failure.

Swift [7] describes the procedures for determining residual strength in the presence of discrete source damage for a number of representative aircraft skin structures. Figure 3 contains an example from Swift's paper dealing with a two-bay longitudinal crack in an aircraft fuselage. The x axis is the size of the lead crack, which is the two-bay crack. The residual strength with the two-bay crack present is represented by the three parallel curves, each of which is based on a different length for the MSD crack.

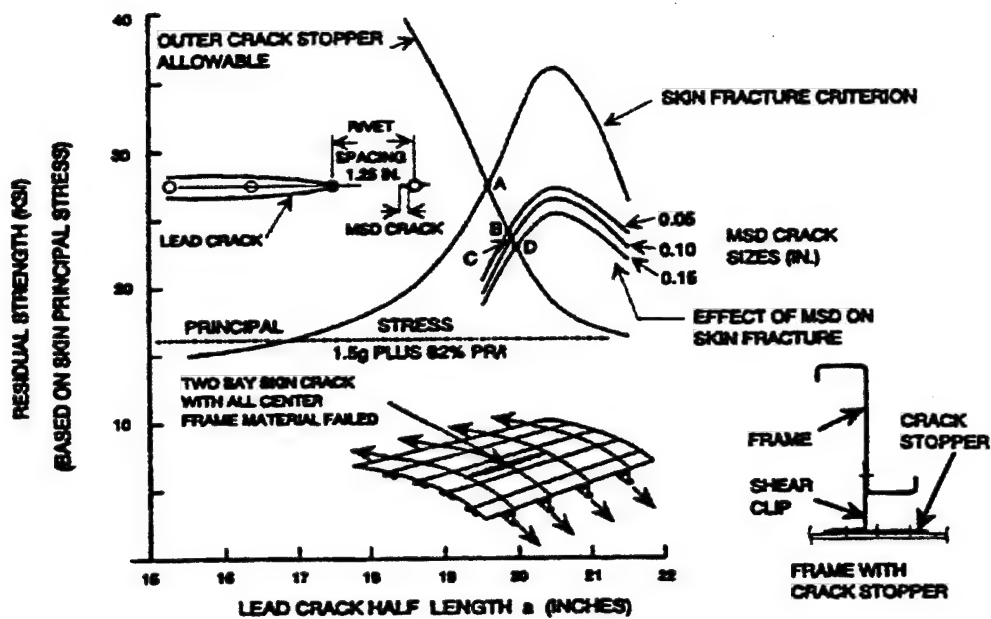


Figure 3. Illustration of Residual Strength Calculation from Swift [7]

With the addition of the residual strength analysis, the computations for the conditional probability of failure, given partial structural failure, are actually less complicated than a standard PROF analysis. A PROF analysis of generalized cracking assumes a normal distribution for material fracture toughness, which adds a dimension to the integral that determines the probability of fracture. The residual strength analysis for DSD is generally too complicated to allow inclusion of the variability in fracture toughness. This is not seen to be a liability, because experience has shown the variability in fracture toughness to be a second-order effect in DSD analyses. The next section provides some details about the calculations performed in a DSD analysis.

3.2 Details of the Approach

The goal in analyzing the effect of WFD in the DSD problem is to evaluate the ability of the structure to complete the current mission when a partial structural failure occurs. This analysis is aimed at one of two or more structural details that interact by providing a fail-safe capability in the event that one or more of the structural details has failed. The evaluation will use the conditional single-flight probability of failure, given that DSD is present as the measure of this ability. The prototype for this analysis is the ability of the structure to survive the sudden appearance of a two-bay crack in the fuselage or wing skin.

The two-bay crack is a crack that spans two bays in the skin, including the stringer or frame between the two bays. The size of two bays is considered an upper bound on the damage that would directly result from penetration of an engine blade thrown from the engine in an uncontained failure or from battle damage. The concern in this damage scenario is whether the crack-stopping structures on either side of the damage will hold through the remainder of the mission. The conditional probability that the crack-stopping structure will fail, given that the DSD has occurred, provides a measure of the ability of the structure to complete the mission.

Since the flaw size distribution changes in time, the PROF DSD analysis should be calculated as a function of time. The presence of DSD only affects the structure during the flight in which it occurs. Therefore, the same model of the growing crack size population that is used in a standard PROF analysis can be used to assess the influence of aging on the conditional probability of failure given DSD. The details of the crack growth model are given in [4]. Because of its severity, DSD, will be detected and repaired before the next flight so that a model of crack growth in the presence of DSD is unnecessary.

The complexity of the load patterns in the presence of DSD would often prohibit the use of the Irwin abrupt fracture criteria for failure. A typical engineering analysis of a structure in the presence of DSD would provide the residual strength (based on average material properties) as a function of the crack size in the remaining structural components. The data requirements for the PROF DSD analysis have been changed accordingly. The variability in fracture toughness is no longer used and the geometry curve has been replaced by the residual strength curve.

The crack sizes that can influence residual strength in the presence of DSD are typically below the current capability of field NDI. Consequently, a PROF DSD analysis would not usually include multiple inspection intervals. The capability to analyze multiple inspection intervals has been retained, however, because the structure was already in the code. The user must supply parameters for the POD function even if inspections are not included in the analysis.

The computation of the single-flight probability of failure for the DSD analysis is similar to the standard PROF analysis. Let $\sigma_R(a)$ represent the residual strength, in the presence of DSD, as a function of crack length. Then the single-flight probability of failure given DSD is given by:

$$\text{SFPOD}(t|D) = \int_0^{\infty} f_t(a) * \bar{H}(\sigma(a)) da, \quad (1)$$

where $f_t(a)$ is the probability density function of flaw size at time t and $\bar{H}(\sigma)$ is the peak load exceedance probability. The main differences are the elimination of the integral across the fracture toughness distribution and the replacement of the functional determination of residual strength based on the geometry curve with a table look-up of residual strength.

Equation 1 is actually a double integral of the joint distribution of crack length and peak stress since $\bar{H}(\sigma)$ is the integral of the probability density function of peak stress from σ to infinity. Figure 4 shows an illustration of the joint density of crack length and peak stress. The curved line across the surface represents the residual strength as a function of crack length. The integral in Equation 1 is the volume under the joint density over the region where stress exceeds residual strength; which is the region labeled "Failure" in the plot.

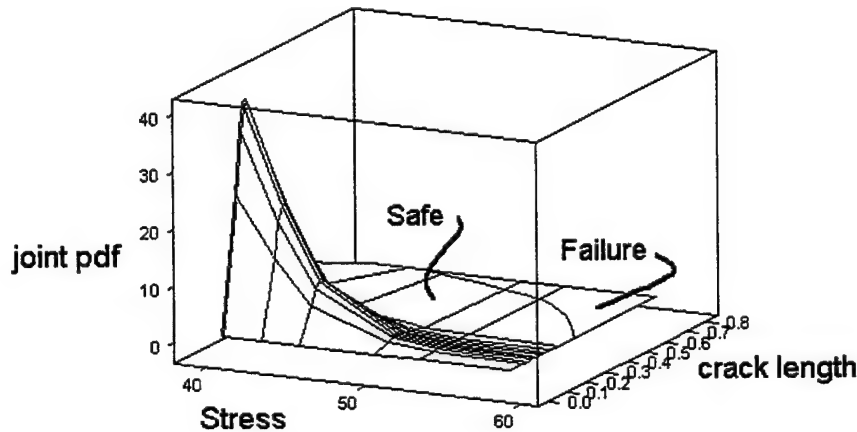


Figure 4. Plot of the Joint Probability Density Function of Crack Length and Peak Stress

The output of the PROF DSD analysis includes a table and a plot of the conditional single-flight probability of failure, given that DSD has occurred as a function of time. The over-

all probability of fracture is the product of the probability of discrete source damage and the conditional probability of failure given DSD has occurred. For a given type of aircraft, there will be a maximum allowable probability of fracture and some estimate of the likelihood of discrete source damage. The maximum allowable conditional probability of failure, given DSD, is the maximum allowable overall probability of failure divided by the probability of discrete source damage. The estimated onset of WFD can then be determined from the time at which the conditional probability of failure reaches the maximum allowable in the PROF DSD analysis output. An example application is given in the following section.

3.3 Example

The data from the B-707 teardown inspection performed as part of the JSTARS assessment will be used to illustrate the procedures for an analysis of the impact of WFD on the fail safety in the presence of DSD. A detailed description of the data and the problems associated with using the B-707 for the JSTARS was given by Lincoln [10]. The example presented here centers on the fail-safety capability of stringer 7 in the lower wing skin after stringer 8 and the adjacent wing panels have failed.

Figure 5 contains a schematic of the B707 wing. The left half of Figure 5 shows the entire structure and the location of stringer 8 (S8). A cross-section of the skin and stringers is shown in the right half of Figure 5. The example will analyze the effect of a break in stringer 8 and the adjacent skins on the large adjacent stringer S7.

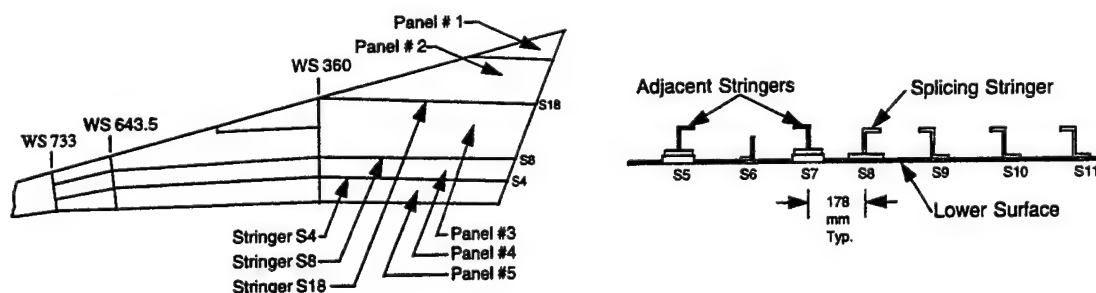


Figure 5. Schematic of the B-707 Wing and Side View of the Skin and Stringer Structure. Taken from Lincoln [10].

The data were collected and the structural analyses were performed by Boeing under an Air Force contract [11]. The data and analysis results were delivered in a series of letter reports and in Excel spreadsheets. The data used for this example were extracted from the spreadsheets.

The structural analyses relevant to the DSD analysis include the crack growth curve, the stress exceedance data in the presence of DSD and the residual strength of stringer 7 in the presence of DSD. Figure 6 contains a plot of the crack growth curve; which was determined for intact structure under normal conditions. The DSD analysis is not concerned with crack growth in the presence of DSD because it is assumed that the DSD will be detected and repaired before the next flight.

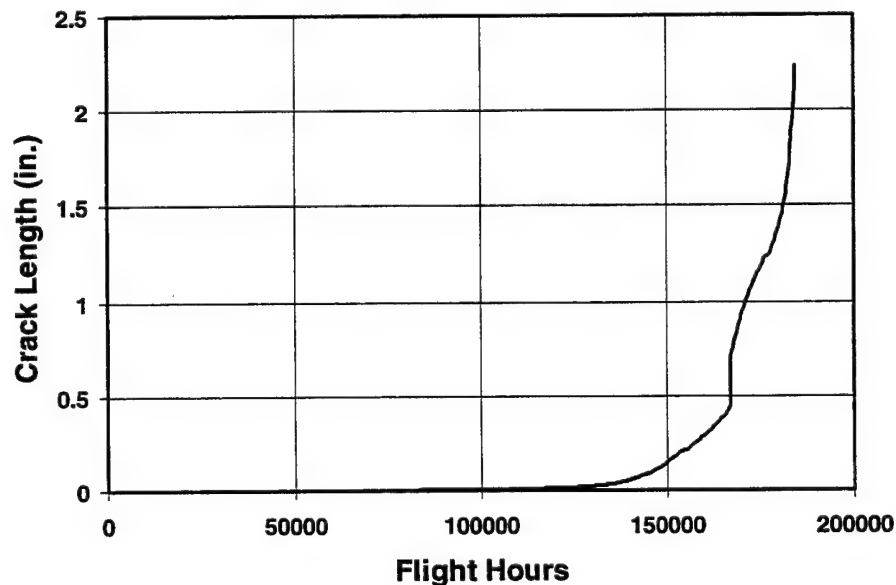


Figure 6. Crack Growth Curve for Stringer 7 with All Structure Intact

Figure 7 illustrates the analysis of the peak load distribution from the exceedance data. The basis for the exceedance data is the spectrum used to generate the crack growth curve. The stresses were transformed to account for the damage to stringer 8 and the adjacent panels to get the empirical stress versus exceedance probability illustrated by the points in Figure 7. The straight line represents the Gumbel distribution that was fit to the data.

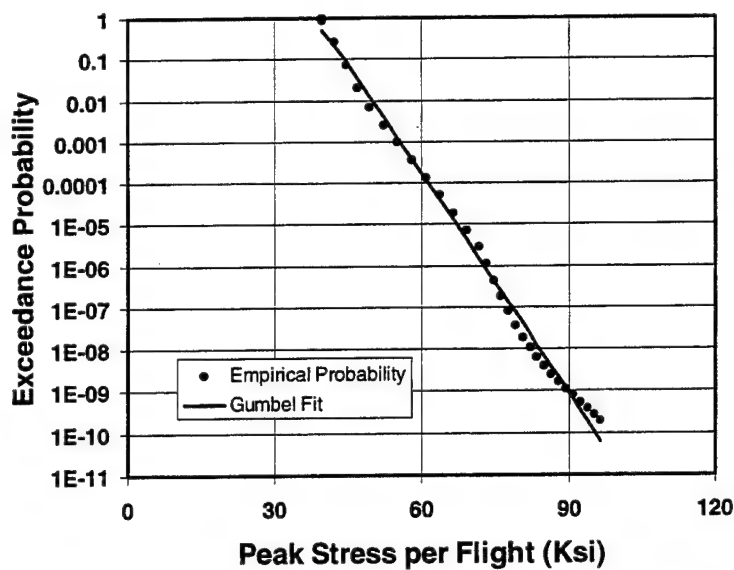


Figure 7. Peak Stress Distribution with DSD Present

The residual strength function is plotted in Figure 8. The shape of the stringer is responsible for the flat region in the residual strength function. The residual strength function was derived primarily from the stress intensity curve for the stringer. Modifications from the Irwin criterion were required at low crack lengths and at the flat region in the middle of the curve. At low crack lengths, the Irwin criterion would push the residual strength to infinity, so it was necessary to truncate the residual strength function to the maximum material strength. The stress intensity factor actually dips between 0.5 and 1.5 inches because of the shape of the stringer. The residual strength does not, however, increase, resulting in the flat region in the residual strength function.

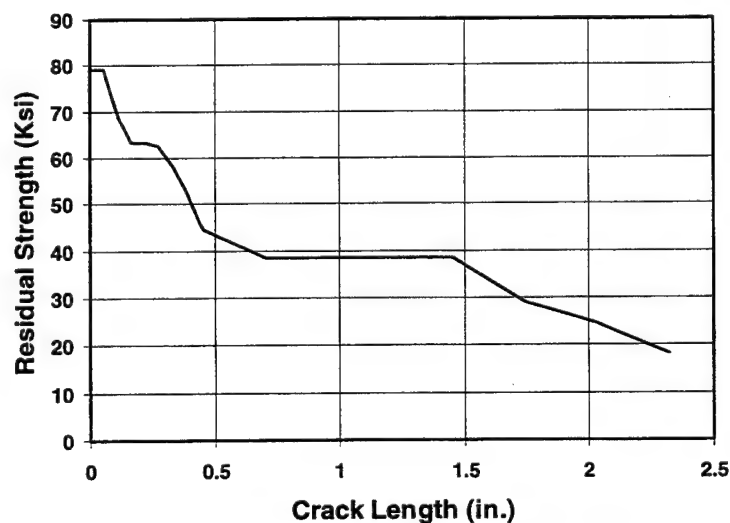


Figure 8. Residual Strength as a Function of Crack Length in Stringer 7

The analysis was performed for two different initial crack length distributions. The crack length data were collected from an aircraft with 57,382 flight hours. The single-flight probability of failure is unacceptably high for the distribution seen in the teardown data. Since many of the JSTARS aircraft will have fewer hours, the distribution was adjusted to an age of 40,000 flight hours. The two-crack length distribution functions are illustrated in Figure 9. A lognormal distribution was fit to the upper tail of the teardown data and the time adjustment was made by back extrapolating the percentiles from the 57,382 distribution using the crack growth curve.

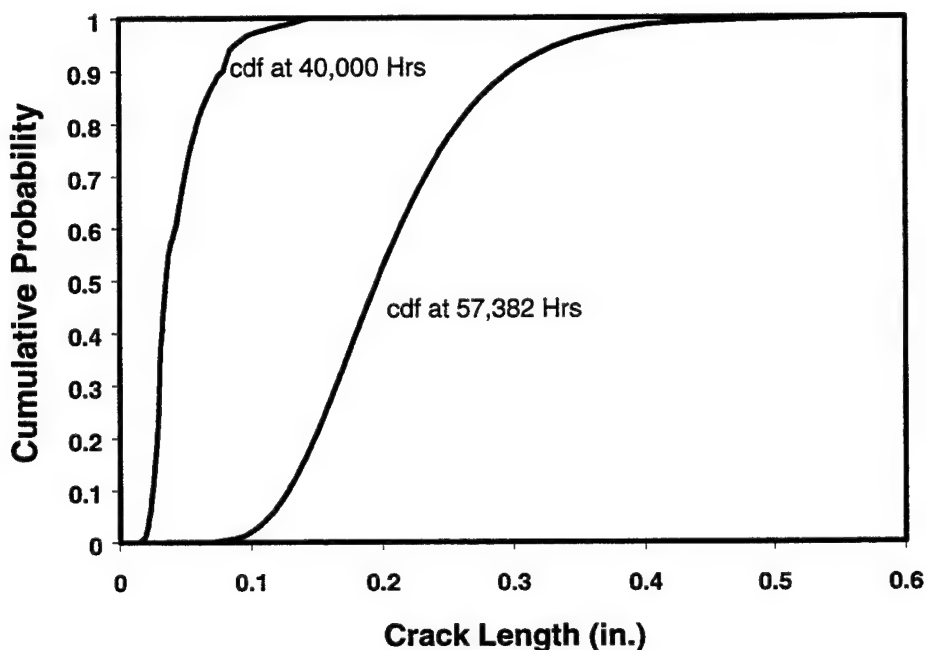


Figure 9. Comparison of the Flaw Size Density Function at 40,000 Hours with the Density Function at 57,382 Hours

The results of two different PROF DSD analyses are plotted in Figure 10. The solid line represents the analysis using the flaw size distribution from the 57,382-hour aircraft as the starting point. The dashed line plots the results from using the flaw size distribution adjusted to a 40,000-hour aircraft. The two curves show close agreement in the overlap; however, some difference is expected since the time points at which calculations are made do not coincide from the two analyses.

Lincoln [10] cited 10^{-7} as the desirable overall single-flight probability of failure and an estimated probability of DSD as 10^{-3} . The resultant requirement for the fail-safe capability of stringer 7 is 10^{-4} . Clearly, the aircraft at 57,382 hours does not meet this requirement. Starting at 40,000 hours, an aircraft will have approximately 16,000 hours before the conditional single-flight probability of failure exceeds the 10^{-4} requirement.

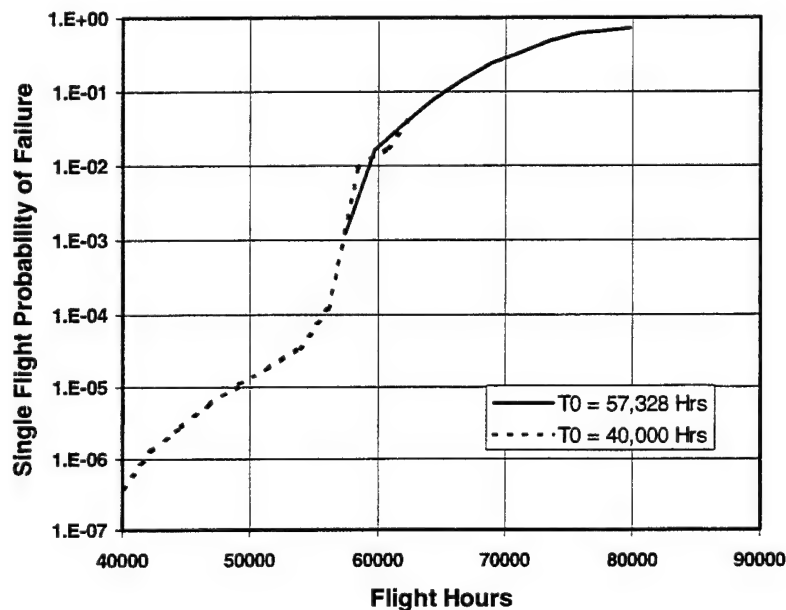


Figure 10. Comparison of Single-Flight Probability of Failure Starting from 57,382 Hours versus 40,000 Hours

The use of the PROF DSD analysis module has been illustrated using data from the B-707 JSTARS aircraft. The problem of evaluating the fail safety capability of lower wing stringers in the B-707 is an example of the prototype DSD analysis. The essential elements that make a problem suitable for the PROF DSD module are:

- 1) interest in the conditional probability of failure, given that adjacent structural elements have failed,
- 2) the likelihood of failure is increased by the presence of MSD,
- 3) a prediction of the growth of MSD cracks with time is available, and
- 4) an analysis of residual strength as a function of MSD crack size is available.

Section 4

Multi-Run Data Management

A single run of PROF produces failure probabilities for the specific population of details being modeled by the geometry and anticipated stresses of the deterministic crack growth model. For example, regions of equivalent stress and geometries are often identified for stress raisers in a fleet of aircraft. When the initiating crack size distribution is representative of all cracks that are present in the stress raisers in the fleet, the failure probabilities would be applicable to a randomly selected airframe from the fleet. There are many structural details for which this calculation is directly relevant and, in fact, decisions to change inspection schedules have been influenced by such risk calculations. However, there are also many structural details for which the conditions are not constant across an entire fleet and the effect of these conditions can be modeled through multiple runs of PROF. When multiple runs are required to adequately model a structure, a method is needed for conveniently managing the data from the multiple runs. This management capability was added to PROF by the introduction of an Excel interface. This section presents the general framework for an analysis of multiple run data that can be applied to many distinct cracking scenarios. Examples are presented for two problems of current interest.

4.1 General Analysis Framework

Many risk analysis scenarios can be formulated in the following analysis framework. The total population of details is divided into sub-populations of equivalent material, stresses and geometries, i.e., into sub-populations of equivalent crack growth properties. Conditional failure probabilities are then calculated for each sub-population. The conditional probabilities can be directly interpreted in terms of the sub-population represented by the conditions. However, when the relative frequencies of occurrence (probabilities) of the conditions are also known, the conditional fracture probabilities can be combined to provide an overall (unconditional) fracture probability as a function of time. This calculation is given by

$$POF(T) = \sum POF(T/C_i) \cdot P(C_i) \quad (2)$$

where $POF(T/C_i)$ is the probability of failure at T , given that condition C_i was used to determine the crack life of the structure and $P(C_i)$ is the probability that condition C_i applies, $\sum P(C_i) = 1$.

The general formulation expressed by Equation (2) can be applied to many risk analysis scenarios as determined by the definition of the structural conditions, C_i . Three examples of such scenarios would be as follows:

- a) A fighter aircraft will experience a random mix of different missions, each of which has a distinct expected stress sequence. The sub-populations would be defined by mission type and a separate PROF run would be made for each. The overall risk to a randomly-selected aircraft of the fleet would be a weighted average of the risks from the individual missions where the weights, $P(C_i)$, are the proportion of flights expected to be flown in each mission type.
- b) The life of a particular lapjoint is determined by the initiation and growth of a lead crack. However, the stress intensity factor for the lead crack depends on whether one or two cracks emanate simultaneously from the same hole. Further, there are different degrees of corrosive thinning in the aircraft of the fleet. A PROF risk analysis would be performed to obtain the conditional failure probabilities for each combination of single or double lead crack and levels of corrosive thinning. The weighting factors, $P(C_i)$, for the calculation of the unconditional failure probability for a random aircraft would be obtained from both the distribution of corrosive thinning at the lapjoint and an estimate of the proportion of times the lead cracks initiate as single or double cracks. This MSD/corrosion example is discussed in Subsection 4.2.
- c) A structural subsystem comprises three elements: a beam cap, a splice fitting, and a chordwise joint. The subsystem fails only when the chordwise joint fails. However, the stress levels on the chordwise joint are dependent on the failed or intact status of the beam cap and the splice fitting. Further, the stresses on the splice fitting increase if the beam cap is failed. A PROF risk analysis for this reasonably complex multi-element damage scenario can be performed by combining PROF runs of all the distinct and relevant combinations of intact and failed structural elements. The weighting factors for combining the individual runs would be obtained from the PROF output of some of the runs. This Multi-Element Damage example is further discussed in Subsection 4.3.

These examples represent only three of the large number of possible scenarios that might require analysis. However, combining multiple PROF runs through Equation (2) is a common thread for all of these essentially distinct problems. To facilitate the implementation of Equation (2), the PROF code was modified to interface with an Excel workbook. Multiple runs are set up on an input sheet and a single execution of PROF performs the analyses for all of the runs. The complete output from each run is stored on a separate sheet. (The complete output from a single run comprises the probability of failure as a function of time at ten equally-spaced increments in the specified inspection intervals and the crack size distributions before and after each inspection.) A "Results" sheet containing only the fracture probabilities from the runs is also generated. Output data management and plotting are now easily accomplished using standard Excel features.

Consideration was given to the inclusion of macros in the Excel spreadsheet to combine the failure probabilities for selected scenarios. Because of the large number of possible scenarios and the broad spectrum of potential outputs, macros were not added. The calculations performed in Excel are quite straightforward when the analyst understands the particular conditional probabilities being combined. The lack of macros should present no difficulties and may prevent misapplications.

The following two subsections present examples of the use of PROF for the Lap Joint MSD/Corrosion example and the Multi-Element Damage example that were discussed above. The multiple missions example would be analogous to, but simpler than, the MSD/Corrosion example.

4.2 Lap Joint MSD/Corrosion Example

The example risk analysis of a lap joint with MSD and corrosion that will be discussed in this report is based on data from a specimen that is representative of a fuselage lap joint. The lap joint specimens had been used in a fatigue test program by Carleton University and the National Research Council (NRC) of Canada [12, 13]. Crack growth predictions for the specimens were performed as part of a program to develop an analytical corrosion damage assessment framework and the specimen test data were used to verify the predictions [14]. The example is presented to demonstrate the risk analysis methodology.

The specimen, Figure 11, is constructed of two 1 mm sheets of 2024-T3 clad aluminum with three rows of 4 mm 2117-T4 rivets (MS20426AD5-5). The rivet pattern has 25.4 mm pitch and row spacing with an edge margin of 9.1 mm. The test specimens were 25.4 cm wide with 8 fasteners in each row across the width.

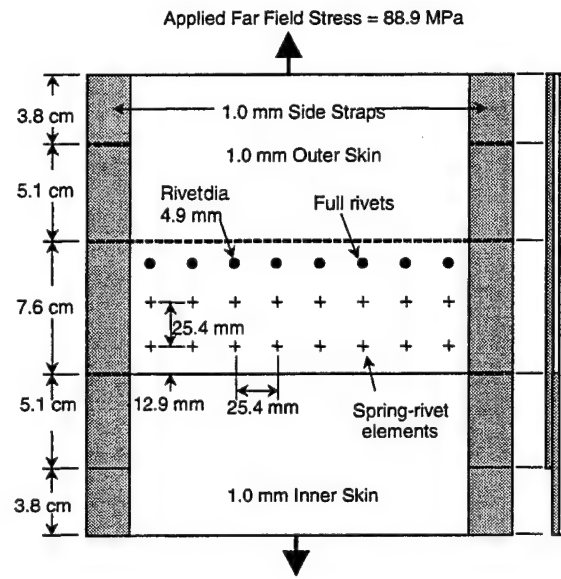


Figure 11. Schematic of Lap Joint Specimen

Constant amplitude fatigue tests had been conducted at Carleton University on the lap joint specimens in non-corroded and corroded conditions with a constant amplitude far field stress of 88.9 MPa with $R = 0.2$. Details of the test procedure and resulting fatigue crack growth data are presented in [13]. Nine non-corroded specimens were tested to failure to provide baseline data for comparison with corrosion specimens. Only data from these non-corroded baseline specimen tests are used in this example. Histories of crack size versus cycles for all cracks that initiated in the top row of rivet holes were recorded during the tests and were available for analysis. Examination of the histories showed that 95 percent or more of the joint life was expended when the lead crack reached about 9 mm and crack growth became unstable. Further, lead cracks initiated in accordance with two dominant scenarios. Scenario 1 is defined as a single crack originating from one side of a central hole. Scenario 2 is defined as approximately simultaneous, diametric cracks originating from both sides of a central hole. Subsequent analysis showed significantly shorter lives for the double initial cracks. Analysis also showed that assuming both cracks were of equal size produced only 5 per-

cent shorter lives than assuming one crack was twice the size of the second. Consequently, the assumptions were made that: a) joint life is determined by the initiation and growth of lead cracks that originate by one of two scenarios; b) the cracks are of equal size in the double crack scenario, and, c) the panel is essentially failed when the lead crack reaches 9 mm.

Because first cracks were simultaneously discovered in different holes in four of the nine data sets, there were a total of 13 lead cracks. Eight were from Scenario 1 and five were from Scenario 2. For this population of structural elements, it was assumed that probability of a randomly-selected lap joint having a Scenario 1 lead crack was 8/13 and the probability of a randomly-selected lap joint having a Scenario 2 lead crack was 5/13.

Crack growth analyses were performed for both scenarios [15]. Stress analysis was performed using FRANC2D/L, a finite element, fracture mechanics analysis code with crack propagation capability [16, 17]. The resulting crack tip stress intensity factor values as a function of crack size were then input to the crack growth code AFGROW [18] for selected degrees of corrosion severity. The no-corrosion, constant amplitude peak stress of the baseline fatigue tests and crack growth analyses was 88.9 MPa with an *R* ratio of 0.2. Predicted cyclic life from 0.25 mm to 9 mm averaged about 30 percent more than the test data.

Corrosion severity was modeled in terms of percent of thinning with the attendant increase in stress. To reflect corrosion severity, crack growth predictions were made for the somewhat arbitrarily selected levels of 0, 2, 5, 8, and 10 percent corrosive thinning by proportionate adjustments of the stress levels.

For the specimen conditions being modeled, the population of lap joint specimens has been divided into sub-populations based on combinations of two MSD scenarios and five corrosion severity levels. Cracking occurred in the two dominant MSD scenarios whose influence on crack growth was exhibited through the stress intensity factor. Corrosion severity was characterized by the metric of uniform thickness loss whose influence on crack growth is exhibited through the experienced stress levels. Each combination of MSD scenario and thickness loss produces a different crack growth analysis so that each combination must be individually analyzed in the risk analysis.

| | | Dominant MSD | | |
|--------------------|----------------------|---------------------|---------------------|---------------------------------|
| Corrosion Severity | Proportion of Joints | Scenario 1 p_1 | Scenario 2 p_2 | Composite over MSD |
| Thickness Loss 1 | q_1 | $POF_{11}(T)$ | $POF_{21}(T)$ | $p_1POF_{11}(T)+p_2POF_{21}(T)$ |
| Thickness Loss 2 | q_2 | $POF_{12}(T)$ | $POF_{22}(T)$ | $p_1POF_{12}(T)+p_2POF_{22}(T)$ |
| Thickness Loss 3 | q_3 | $POF_{13}(T)$ | $POF_{23}(T)$ | $p_1POF_{13}(T)+p_2POF_{23}(T)$ |
| Thickness Loss 4 | q_4 | $POF_{14}(T)$ | $POF_{24}(T)$ | $p_1POF_{14}(T)+p_2POF_{24}(T)$ |
| Thickness Loss 5 | q_5 | $POF_{15}(T)$ | $POF_{25}(T)$ | $p_1POF_{15}(T)+p_2POF_{25}(T)$ |

$POF_{ij}(T) = POF(T/S_i, L_j) =$ Probability of failure for Scenario i , Thickness Loss j

p_i = Proportion of lap joints with crack initiating under Scenario i

q_j = Proportion of lap joints with uniform thickness loss at level j

Figure 12. Conditional Failure Probabilities for 2 MSD Scenarios and 5 Levels of Uniform Thickness Loss

Figure 12 illustrates the partitioning of the total population of the lap joints into the ten sub-populations. Every lap joint must fit into one of the sets of conditions defined by MSD scenario and thickness loss. The probability that cracks will initiate under Scenarios 1 and 2 are p_1 ($=8/13$) and p_2 ($=5/13$), respectively. The probability that a randomly-selected lap joint will have uniform thickness loss level j is q_j . $POF(T/S_i, L_j) = POF_{ij}(T)$ is the probability of fracture as a function of time for the combination of MSD Scenario i and Thickness Loss j . The calculation of the unconditional probability of failure for a random lap joint in the fleet for each corrosion severity level is shown in the last column. An analogous calculation could be performed across severity levels to obtain composite failure probabilities for each MSD scenario.

An interpretation of the corrosion effects can be made directly from the PROF output. If an estimate of the distribution of thickness loss in the fleet is also available, the results of the individual runs of PROF can be combined using Equation (1) to provide an overall fracture probability for a randomly-selected detail. Further, the distribution of time to reach a fixed fracture probability can be inferred from the percentiles associated with the corrosion severity levels. These analyses will be demonstrated for corrosion in a representative lap joint.

It is realized that the risk analysis discussed herein does not account for the stress levels increasing as a result of increasing corrosion over the analysis period. At present, there are no accepted models for the corrosion damage growth (thickness loss) as a function of time so that the crack growth calculations are based on the state of corrosion at the beginning of the analysis interval. In reality, the stresses in the spectrum should be slowly increasing. If this effect could be accounted for in the deterministic analysis, the crack growth data input to PROF would reflect the change. However, the peak stress distribution would need to be made more severe at discrete increments. This added complexity could also be introduced by adding the additional level of conditioning and performing multiple PROF runs for each of the other ten conditions. This added level of conditioning provides insight into the total number of different runs that might be required to completely analyze a structure.

It might be noted that in the lap joint example of this paper, the peak stress distribution had no effect on the failure probability. The failure of the joint specimen was determined by reaching an unstable crack growth state when the lead crack reached 9 mm, a size far below the critical crack size for the applied far field stress.

4.2.1 MSD/Corrosion Example PROF Input

The risk analysis for the lap joint corrosion example requires ten individual runs of PROF – two MSD scenarios and five stress levels for each of the MSD scenarios. The most significant inputs for the runs of this lap joint example are the crack growth projections and the initial crack size distribution. The other PROF inputs that reflect the changes between runs are the table of stress intensity factor divided by stress (K/σ) as a function of crack size and the distribution of peak stresses. These were changed between runs even though they had no affect on the results. K/σ came from the FRANC2D/L analysis. The peak stress distribution was estimated by a Gumbel extreme value distribution that had a mean at the appropriate constant amplitude level and a very small standard deviation to reflect the constant amplitude nature of the tests. Fracture toughness for the specimen was assumed to be normally distributed, with a mean and standard deviation of 152 and 11.4 $\text{Mpa}\sqrt{\text{m}}$, respectively. Because the example being modeled does not include inspection and repair cycles, reasonable, but arbitrary, data were used to define the inspection capability and the equivalent repair flaw size distributions.

The AFGROW crack growth curves for Scenarios 1 and 2 are presented in Figures 13 and 14, respectively. Each figure contains five crack growth curves reflecting the five levels of corrosion severity. The shorter crack growth lives from Scenario 2 are apparent from a comparison of these figures.

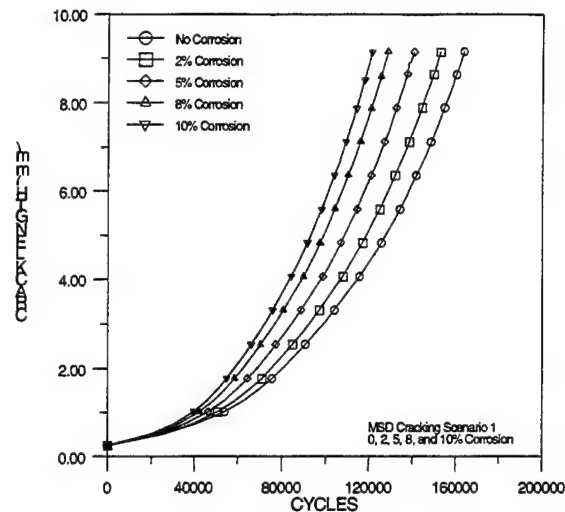


Figure 13. Crack Size versus Cycles for Scenario 1

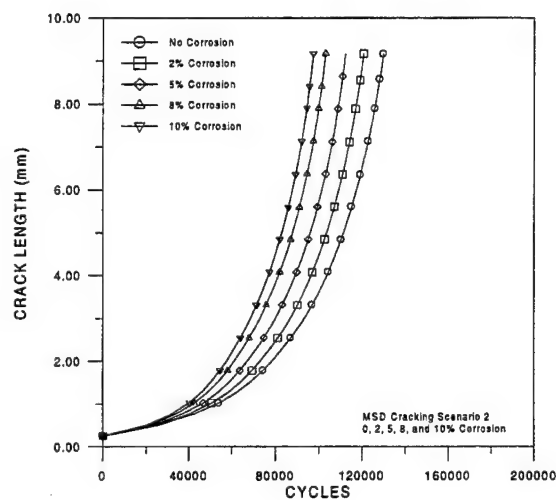


Figure 14. Crack Size versus Cycles for Scenario 2

The initiating flaw size distribution was generated by back calculating from the sizes of the first observed lead cracks and their corresponding ages in the specimen test data. The back calculation was performed in two steps. First, the no-corrosion crack size versus cycles data of Figures 13 and 14 were used to determine the time at which each lead crack would have reached

0.25 mm. An exponential growth model was then fit to each lead crack to estimate an equivalent crack size at 50,000 cycles. Note that the inverse of this process returns each of the observed lead cracks to its original size and cycles.

The times to reach 0.25 mm for the cracks from the two MSD scenarios were statistically indistinguishable. Similarly, there was no statistical difference between the equivalent lead crack sizes from the two MSD scenarios at 50,000 cycles. The two sets of data were pooled to obtain the initiating flaw size distribution. The equivalent crack sizes at 50,000 cycles were fit with a mixture of two Weibulls as shown in Figure 15. Also indicated in Figure 15 are the MSD scenarios of origin of the lead cracks.

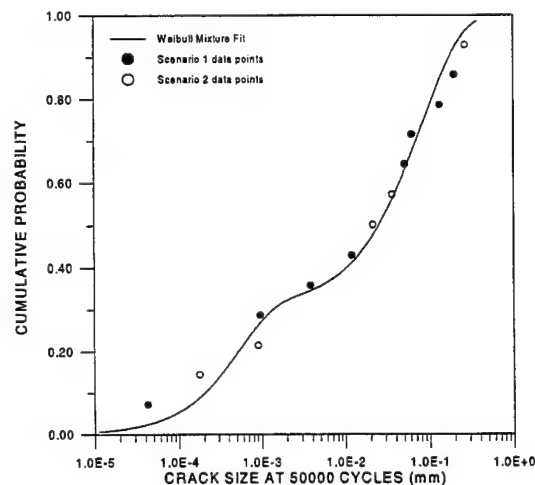


Figure 15. Weibull Mixture of Initial Crack Sizes

4.2.2 MSD/Corrosion Example PROF Results

Probability of failure as a function of cycles was calculated for each of the ten combinations of cracking scenario and corrosion severity. Failure of the lap joint specimens was defined as the lead crack exceeding 9 mm, as previously discussed. Figures 16 and 17 present the failure probabilities as a function of experienced cycles for Scenarios 1 and 2, respectively. The failure probabilities behave as expected with increased risk of failure at a fixed age for Scenario 2 as compared to Scenario 1, and increasing risk of failure as the stress level increases due to corrosion material loss. These calculations do not account for any additional corrosive thinning after the start of the analysis.

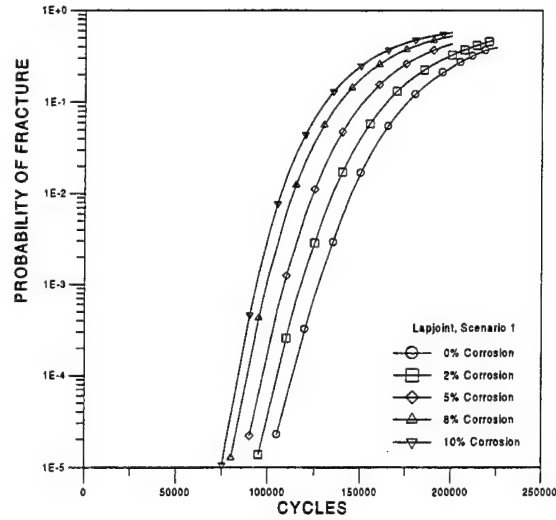


Figure 16. POF versus Cycles for Scenario 1

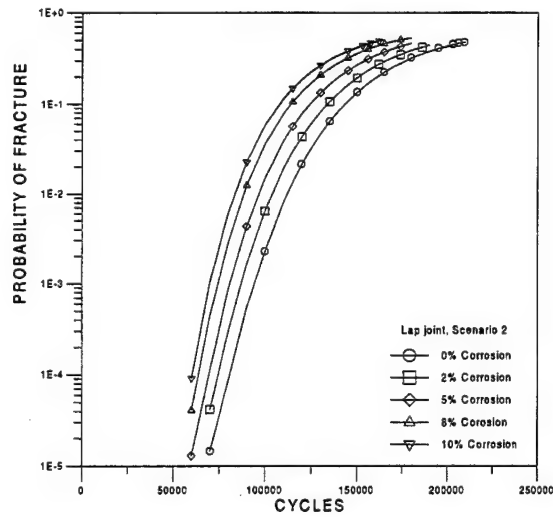


Figure 17. POF versus Cycles for Scenario 2

As a gross check on the capability of the risk analysis methodology, Figure 18 compares the calculated probability of failure as a function of cycles for 0% corrosion for Scenarios 1 and 2 to the observed distributions of failure times. Superimposed on the predicted failure probabilities are the observed cumulative distributions of the cycles to failure from the lap joints that were the basis of the analysis. The observed cumulative distribution function was obtained by ordering the cycles to failure and dividing the ranks of the ordered times by the sample size plus one. That is,

$$F(T_i) = i/(n+1) \quad (3)$$

where i is the rank for T_i , the time at which the i^{th} crack exceeded 9 mm, and n is the number of observed cracks that met the definition for the scenario. Sample sizes for Scenarios 1 and 2 were eight and five, as noted earlier. The differences between the observed and predicted probabilities of failure are most likely due to the conservative deterministic life predictions or the extrapolation of the crack-size-versus-cycles relation that was required to obtain the initiating distribution of crack sizes.

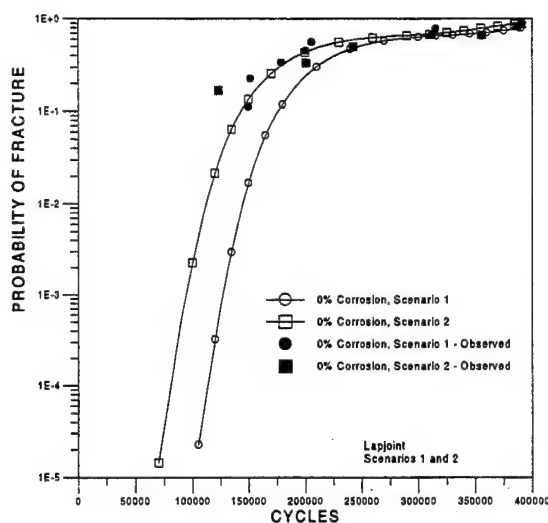


Figure 18. POF versus Cycles for Scenarios 1 and 2 Showing Comparison with Observed Data

Figures 16 and 17 presented the conditional failure probabilities given the respective cracking scenario. The unconditional failure probability for a lap joint chosen at random from the population being analyzed is calculated as a weighted average of the conditional probabilities where the weighting factors are the proportion of specimens which will initiate cracks in the two scenarios. See Equation (2) and Figure 12. The weighting factors were estimated from the lap joint data in which 8 of the 13 lead cracks were from Scenario 1 (initial lead crack from one side of the hole) and 5 of the 13 were from Scenario 2 (initial lead crack from diametrically-opposite sides of the hole). Thus, $p_1 = 8/13$ and $p_2 = 5/13$. Using these factors, a comparison of the observed and predicted cycles to failure for the composite of the two scenarios without corrosion is shown in Figure 18. Again, the difference between the predicted and observed distributions of cycles to failure displays the somewhat non-conservative risks of the predicted failure probabilities.

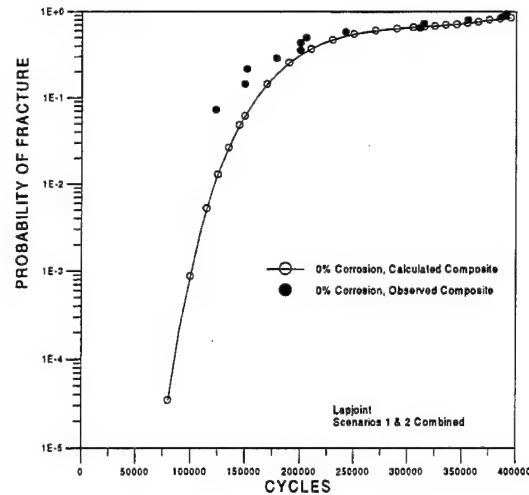


Figure 19. POF versus Cycles for Composite of Scenarios 1 and 2 Showing Comparison with Observed Data

Figure 20 summarizes the probabilities of failure for a randomly-selected lap joint that can have either MSD scenario and is subject to the expected stress history for five levels of corrosion severity. These results will be interpreted both in terms of the times to reach a defined probability of fracture (POF) and in terms of the relative differences in POF at a fixed number of cycles.

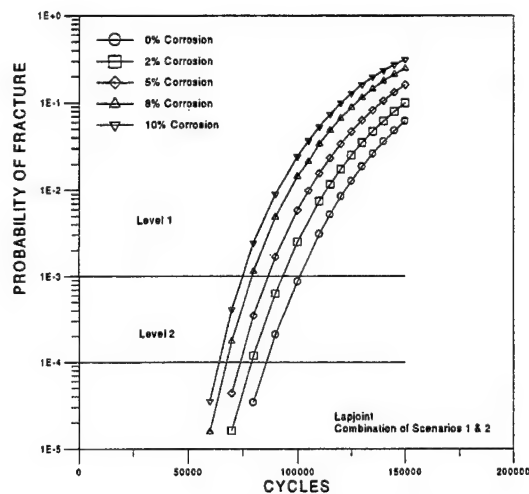


Figure 20. POF versus Cycles for Scenario Composites

The cycles to reach a fixed POF for the different degrees of corrosion severity can be read from Figure 20 as indicated, for example, at POF equal to 0.001 and 0.0001. Assume that the proportion of lap joints in the population that contain each of the five degrees of corrosion is known. Then the distribution of the time to reach the POF levels can also be inferred. To illustrate, three

representative distributions of corrosion damage were assumed, as given in Table 1. Mix 1 is symmetric about a five percent material loss. Mix 2 is representative of a more severely corroded population. Mix 3 is representative of a less severely corroded population and is considered to be more representative of the corrosion that would be expected in aircraft. Figure 21 presents a histogram of Mix 3. The corresponding percentage of lap joints would be expected to reach the selected POF level in the indicated number of cycles. The histogram for cycles to reach $POF = 0.0001$ for severity Mix 3 is shown in Figure 22. The cumulative distribution of time to reach the two POF levels for the three distributions of corrosion severity are shown in Figure 23.

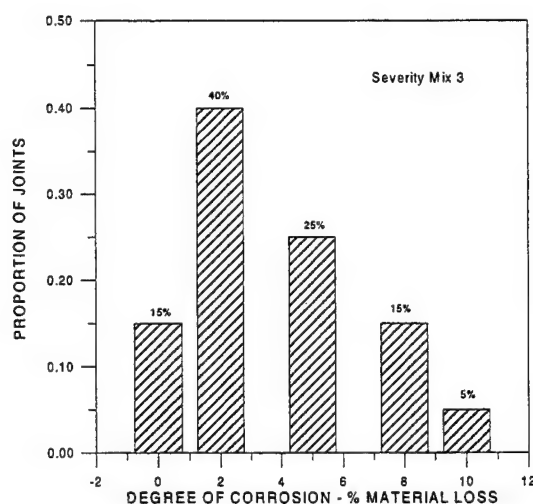


Figure 21. Example Histogram of Levels of Corrosion Damage – Severity Mix 3

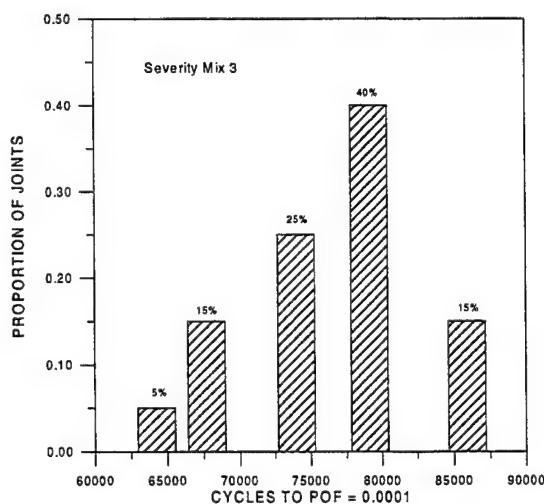


Figure 22. Example Histogram of Cycles to $POF = 0.0001$ – Severity Mix 3

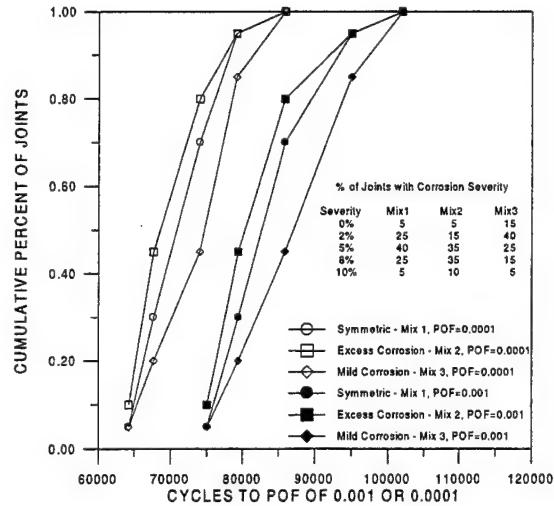


Figure 23. Cumulative Distribution of Cycles to Selected POF – 3 Corrosion Severities

At a fixed number of cycles, the failure risk of a corroded lap joint can significantly exceed that of a non-corroded lap joint. To illustrate this difference, Figure 24 presents the ratio of failure probabilities for each of the four degrees of corrosion severity to that of the non-corroded lap joints. The ratios are presented as a function of the failure probability of the non-corroded lap joint. The lap joint failure probability for the severity characterized by ten percent thinning can be 70 times greater than that of a non-corroded lap joint. If maintenance scheduling were based on keeping the failure probability below about 0.0001 to 0.001, a lap joint with ten percent corrosion thinning would have a 25 to 50 times greater chance of resulting in fracture.

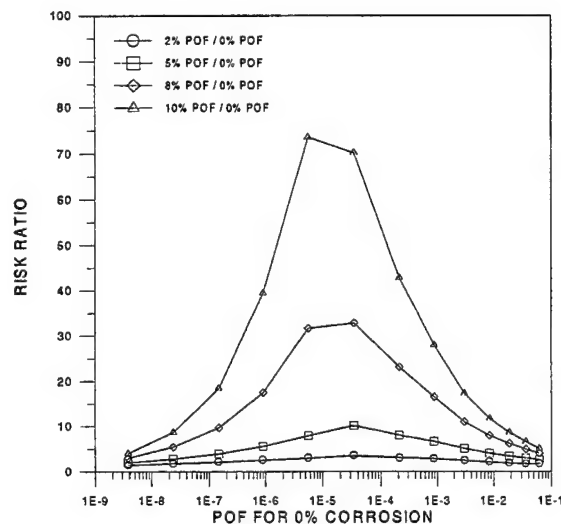


Figure 24. Risk Ratios Normalized to No Corrosion Condition

4.2.3 MSD/Corrosion Example Summary

This example demonstrates that it is possible to extend PROF to include probabilistic descriptions of the factors which influence fatigue life. In particular, a risk analysis was performed for fatigue failures in a representative lap joint in which the crack growth calculation was influenced by corrosion thickness loss and two scenarios of MSD. The basic approach to the analysis was to use deterministic crack growth calculations for different percentiles of the influencing factors in the probability of failure calculations, yielding conditional probabilities of failure. The full use of the analysis assumed that estimates of the proportion of Scenarios 1 and 2 and an estimate of the proportion of lapjoint with the discrete level of corrosive thinning were available, so that the conditional failure probabilities can be combined or otherwise interpreted.

In the lap joint example of this paper, the relative frequency of the two dominant MSD scenarios was estimated from data from a test program of the modeled specimen. Example distributions of thickness loss were assumed to demonstrate the calculations and interpretation. For this example, a ten percent thickness loss increased the failure probability by a factor of as much as 70 over the no-corrosion condition. Depending on the consequences of failure, inspection intervals based on the no-corrosion stress levels could pose a safety issue to corroded joints. The results were also used to demonstrate the generation of the distribution of time to a fixed risk.

4.3 Multi-Element Damage Example

In the multi-element damage scenario, two or more structural elements bridge the same load path and the damage states of the elements can interact. In this scenario, failure of selected combinations of elements may not lead to system failure, but the effects of the failures may well lead to changes in the fracture mechanics (loads or geometry factors) of the remaining elements. Thus, the probability of system failure changes when the non-critical elements fail and to evaluate the failure risks of the complete structure, the functional interaction of the structural elements must also be taken into account. PROF can provide a reasonable approximation to this potentially-complex calculation through the general analysis framework of Subsection 4.1.

A fault tree type of analysis is first performed to identify all of the interactive states that have an affect on the conditions leading to system failure. This step is performed external to PROF

and may prove to require extensive stress and fracture mechanics analyses. These states will represent structural conditions that can be modeled by deterministic crack growth analysis. PROF can then be used to calculate the conditional probability of failure, given the potential combinations of failed and unfailed states of the elements. The unconditional failure probability of the complete structure is a weighted average of the conditional probabilities where the weights are the probabilities of being in each of the states, i.e., the probability that selected elements will have failed.

It is apparent that there are, potentially, a very large number of possible combinations of structural elements that would need to be considered in the analysis of a complex structure. From the viewpoint of structural interaction, it is judged that three or four elements will suffice. For two elements, there are only two basic combinations: the structure will fail if either element fails (the elements are in series), or the structure will not fail if one of the elements fails (the elements are in parallel). Note in the latter case, that the crack growth properties of either element will change upon failure of the other. Even this simple multi-element structure may require three PROF runs to be combined. If there are three interacting elements, there are a total of five basic combinations of series and parallel arrangements, and many more potential analysis combinations that could require PROF runs. These runs are easily combined using the Excel interface.

An example problem is the best approach to understanding the methodology for the Multi-Element Damage scenario. The following example is taken from a report on a risk analysis of Wing Station 405 (WS405) of the C-141 aircraft [19].

4.3.1 WS405 Problem Statement

Failure occurs at WS405 in the C-141 airframe when the chordwise joint fractures. Since the stress levels and crack growth behavior in the chordwise joint are dependent on the intact or failed status of both the splice fitting and the beam cap, the risk analysis for WS405 must combine conditional fracture probabilities for the relevant combinations of the states of the structural details. The probability of failure at this wing station under routine operations was previously calculated by Lockheed Aeronautical Systems Company (LASC) for a single inspection interval at 31,000 spectrum hours using a Monte Carlo analysis, [20]. The data were re-analyzed to demonstrate that PROF could be used to calculate the failure risks for the same scenario.

The input required by PROF were provided by LASC from their evaluation of the failure risks at WS405. The input data that were used in the analyses are presented in discussed in detail in [19 and 20].

LASC performed extensive finite element analyses of the chordwise joint, splice fitting and beam cap at WS405 of the C-141 airframe. The intact or fractured status of the beam cap affects the stress levels in both the splice fitting and the chordwise joint. The intact or fractured status of the splice fitting also affects the stress levels in the chordwise joint. Thus, different crack size versus hours relations and different maximum stress per flight distributions are needed for the various combinations of intact and fractured beam caps and splice fittings.

Since structural failure at WS405 of the C-141 airframe occurs when the chordwise joint fractures, LASC established a fault tree, Figure 25, which isolated the fracture events that need to be evaluated in the calculation of the probability of failure of WS405, [20]. The fault tree of Figure 25 was restructured to demonstrate that the WS405 failure probability can be modeled as a weighted average of the probability of fracture of the chordwise joint, given the intact or failed status of the splice fitting and the beam cap. The weighing factors are the probabilities of the intact or fractured status of the splice fitting and the beam cap. The chordwise joint fracture can also be visualized in terms of the Venn diagram of Figure 26 in which the event is partitioned four mutually-exclusive sub-events.

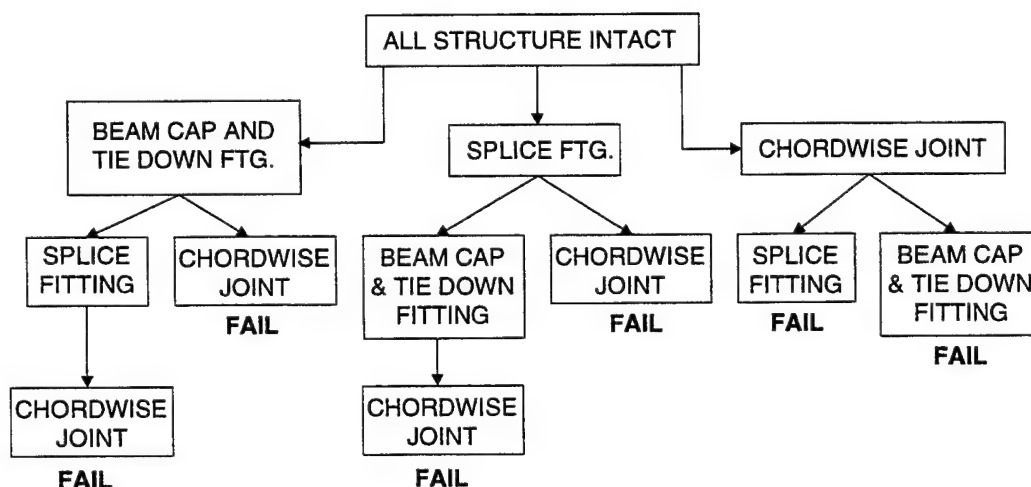


Figure 25. WS405 Fault Tree

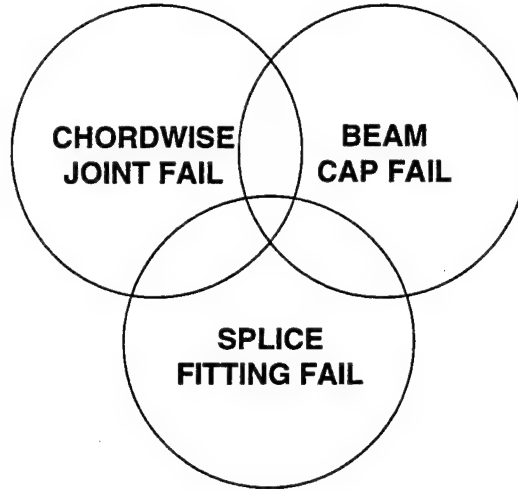


Figure 26. WS405 Venn Diagram

The probability of failure at WS405 (POF) is given by:

$$\begin{aligned}
 \text{POF} &= P\{CSF, SFTAC, BCTAC\} + P\{CSF, SFTAC, BCF\} \\
 &\quad + P\{CSF, SFF, BCTAC\} + P\{CSF, SFF, BCF\} \\
 &= P\{CSF \mid SFTAC, BCTAC\} \cdot P\{SFTAC\} \cdot P\{BCTAC\} \\
 &\quad + P\{CSF \mid SFTAC, BCF\} \cdot P\{SFTAC\} \cdot P\{BCF\} \\
 &\quad + P\{CSF \mid SFF, BCTAC\} \cdot P\{SFF\} \cdot P\{BCTAC\} \\
 &\quad + P\{CSF \mid SFF, BCF\} \cdot P\{SFF\} \cdot P\{BCF\}
 \end{aligned} \tag{4}$$

where

CSF = chordwise joint fracture

$SFTAC$ = splice fitting intact

SFF = splice fitting fractured

$BCTAC$ = beam cap intact

BCF = beam cap fractured

$P\{A, B, C\}$ = Probability of events A and B and C

$$= P\{A \mid B, C\} \cdot P\{B\} \cdot P\{C\}$$

$P\{A \mid B, C\}$ = Conditional probability of event A given the events B and C

Note that because of the effect of the failed or intact effect of the beam cap on the splice fitting that

$$P\{SFF\} = P\{SF \mid BCTAC\} \cdot P\{BCTAC\} + P\{SF \mid BCF\} \cdot P\{BCF\} \tag{5}$$

Further ,

$$\begin{aligned} P\{SFTAC\} &= 1 - P\{SFF\} \\ P\{BCTAC\} &= 1 - P\{BCF\}. \end{aligned} \tag{6}$$

Time histories of the conditional probability of chordwise joint fracture given the intact or failed status of the splice fitting and beam cap were calculated using PROF (with the appropriate α versus T and maximum stress per flight distribution). Similarly, the time histories of the probability of the splice fitting and beam cap being in an intact or failed status were also calculated using PROF. These numbers were combined to calculate the unconditional probability of WS405 failure.

4.3.2 Selected WS405 Risk Analysis Results

PROF computed the single flight probability of fracture at ten approximately equally spaced times throughout each usage interval. The usage intervals were specified in terms of spectrum hours from the zero reference time ((31,000 spectrum hours in this example) and define the times at which the inspection and repair actions are taken. In this risk evaluation at WS405 of the C-141, the analyses were performed over two usage intervals of 328-hour duration. The reported analyses were run assuming an inspection at the start of the analysis (Reference time $T = 0$ or 31000 spectrum hours).

PROF also calculates interval probability of fracture, but only at the end of a usage interval. For the structural elements and conditions of this example, the probability of fracture was dominated by cracks reaching unstable size (about 1 in.) as opposed to an encounter of a maximum stress in a flight. That is, the probability of fracture was determined primarily from the distributions of crack sizes. As a result, the single flight and interval probability of fracture were equal (to three significant figures) for the chordwise joint and the beam cap. The interval probabilities of fracture for the splice fitting were about five percent greater than the single flight fracture probabilities. Therefore, in this application, the single-flight fracture probabilities were used for the probabilities of intact and fractured status of the splice fitting and beam cap, Equation (4), in calculating the unconditional probability of failure at the ten times in a usage interval. This assumption is expected to occur in problems of interest because of the relatively small failure probabilities risks in any realistic problem.

A sample of the results from the WS405 analysis are as follows: Figure 27 presents the probability of fracture as a function of spectrum hours for the splice fittings and the beam caps. This analysis assumed that maintenance (inspection and repair of detected cracks and failures) was performed at $T = 0$ (31,000 spectrum hours) and a subsequent maintenance was performed at 328 hours. The figure displays the relatively high fracture probabilities for the splice fittings, even after the maintenance cycle. In the original data, approximately 75 percent of the beam caps were in a failed crack size state and these were repaired before the failure probability calculations were started. The inspection capability assumed in the analysis was not sufficient to find and repair the cracks in the splice fittings. The effect of the failed beam cap on the fracture probability of the splice fitting was relatively minor in comparison to other effects.

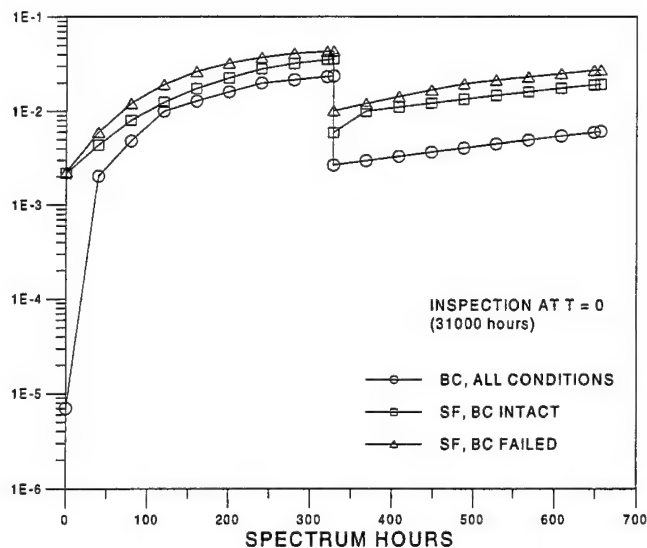


Figure 27. Failure Probabilities of Splice Fitting and Beam Cap

Figure 28 presents the conditional probability of failure of the chordwise joint, given the intact or fractured status of the splice fitting and beam cap. The unconditional failure probability is a weighted average of these conditional probabilities, with the weights being determined by the proportion of intact and failed splice fittings and beam caps. Figure 29 displays the chordwise joint (system) unconditional failure probability along with the conditional failure probabilities. With the inspection at time zero, the intact or failed status of the splice fitting and beam cap had relatively minor effect on the failure probability of the system. Figure 30 compares system

probabilities of failure for the analyses with and without an inspection at time zero. The effect of the maintenance action decreases the failure risks by about a factor of five.

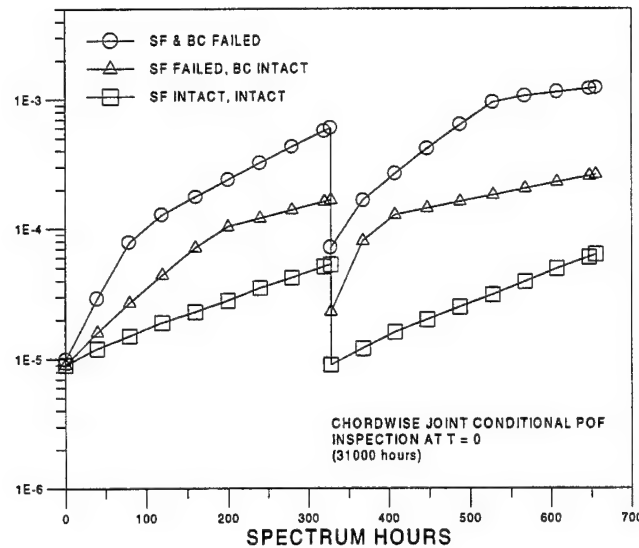


Figure 28. Conditional Failure Probabilities of Chordwise Joint

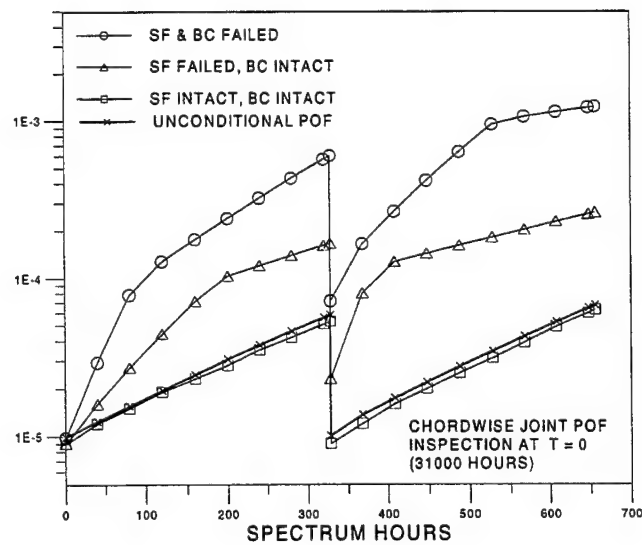


Figure 29. Unconditional Probability of Failure of Chordwise Joint

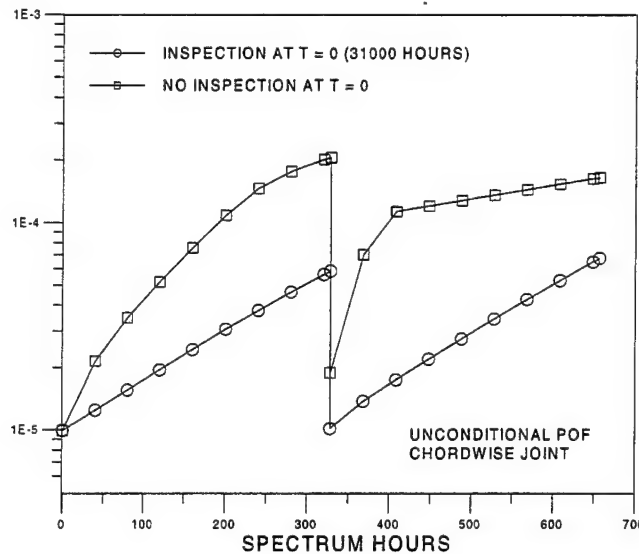


Figure 30. Unconditional Probability of Failure of Chordwise Joint – With and Without Initial Inspection/Repair

4.3.3 Multi-Element Damage Example Summary

The computer code PRobability Of Fracture, PROF, was used to evaluate the probability of failure at WS405 of the C-141 aircraft. Failure occurs at this location when the chordwise joint fails. The stress levels experienced by the chordwise joint are dependent on the failed or intact status of the splice fitting and the beam cap. This multi-element analysis was calculated in terms of the failure probability of the chordwise joint, given the status of the splice fitting and the beam cap, and the probabilities of the condition of the splice fitting and beam cap. The probability of failure at WS405 was calculated for a set of conditions comparable to those used in an independent analysis performed at LASC. For these conditions, the probability of a failure at WS405 in one wing was less than $2 \cdot 10^{-4}$ during a period of 656 hours of operational usage with an inspection/repair cycle at 328 hours.

The example demonstrates that PROF can be used to evaluate the fracture risks associated with more complex structures than the single-stress raiser, which is the current basis of the calculations. The computations for combining the conditional failure probabilities of the elements was easily accomplished in the Excel spreadsheet.

Section 5

Additional Modifications to PROF

Modifications to PROF include changing from FORTRAN to C++, converting the user interface to use Microsoft Foundation classes, improving the numerical methods, and adding an Excel spreadsheet interface for parameter description and tabular output.

Appendix A is a users' manual for PROF. Appendix B details the mathematical aspects of the numerical methods used by PROF. Appendix C documents the source code. Appendix D is the list of PROF source files.

5.1 User Interface

The original version of PROF was written in FORTRAN and is documented in [4,5]. By 1995, a windowed, graphical front-end was added to PROF [6]. The resulting program was called WinPROF. The approach taken for WinPROF was to use the Zinc Application Framework libraries (Ver. 3.5), [see <http://www.zinc.com>]. Zinc is a user interface class library that is designed to be a replacement for Application Program Interfaces (API) such as Microsoft Foundation Classes (MFC) or Unix X/Motif. Its appeal is cross-platform uniformity. However, there are several problems with the use of third-party user interface libraries. They add another layer of application software to a product. They generally do not have exactly the same look-and-feel as programs written directly for a given platform. They are not as responsive to platform changes in user-interface style.

The new version of PROF (PROFv2) eliminates the use of the Zinc Application Framework. The user interface was rewritten to use only MFC. This gives an appearance much closer to other Windows programs. For example, files are opened and closed using the common dialog boxes provided by Windows. These are the same dialogs used by Microsoft Office applications and most commercial applications. Zinc provided its own dialog boxes, which was required to maintain platform independence.

The major component in Zinc that was not present in MFC was a class devoted to plotting. This capability was developed, based on earlier plotting programs written internally at UDRI.

Microsoft has a standard platform for programming, called the Developer Studio. This platform includes an editor, project builder, and debugger. Application frameworks can be developed using the "Application Wizard". The wizard allows standard features of the Windows environment to be included in custom applications. The same Studio environment is used for C++, Fortran, and Java.

The Application Wizard is designed around Microsoft's document-view architecture. The structure of PROF was modified to fit within this document-view organization. A PROF document, for example, contains the same information previously found in the ASCII input file used by WinPROF. The document class contains the input parameters and variables used by PROF. A PROF view is the screen display of PROF document parameters and analysis results.

Currently, the new PROF uses the Single Document Interface (SDI). A screen example is shown in Figure 31. There are four sub-windows or panes, one pane of control buttons, two panes for plots and one pane for text.

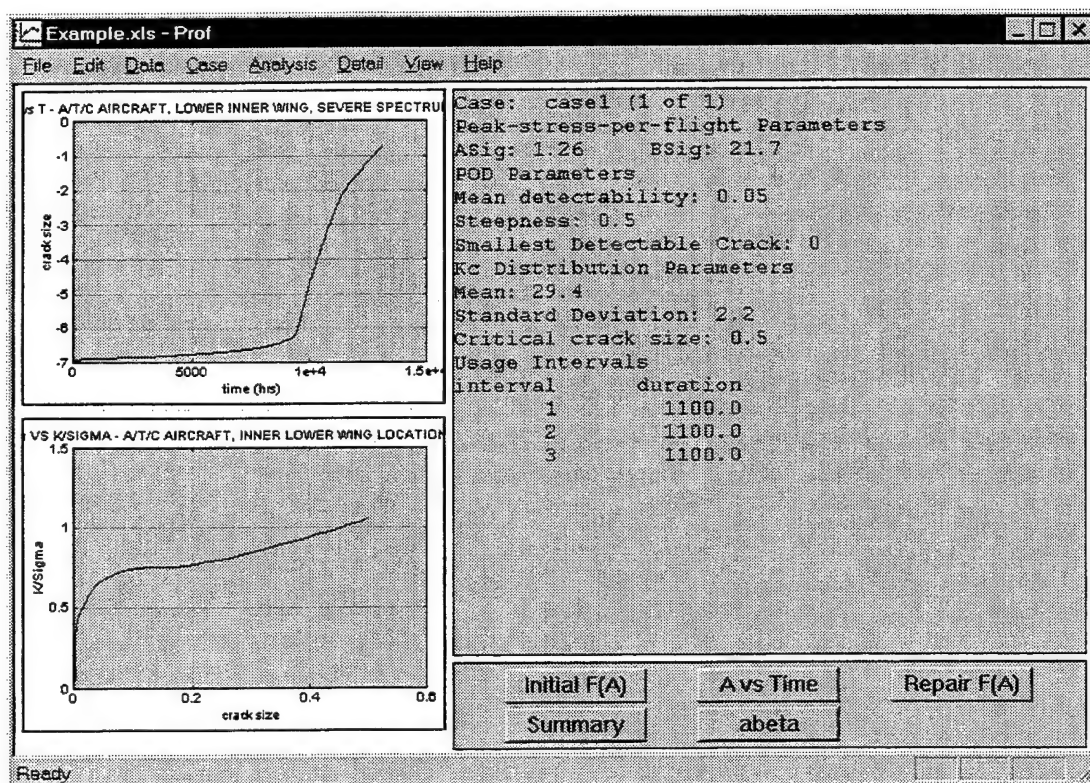


Figure 31. Screen Layout for New Version of PROF

5.2 Excel Interface

The new version of PROF uses Excel spreadsheet files as its documents. The input parameters for a PROF data set were previously stored in an ASCII file (with an .ipt extension). Now they are stored in an Excel workbook document, on a worksheet named Input. Figure 32 shows an example of the input format. The results of a PROF analysis are written as separate worksheets in the same Excel file. Problems with multiple variations can be expressed in one workbook. The input parameters are arranged in columns. Each column is a separate case. During analysis, the results of each case are written on separate worksheets.

There are a number of advantages in using Excel documents. Excel is part of Microsoft Office, which means that it is almost universally available on office computers. Spreadsheet programs have become as familiar a tool for numerical documents as word processing programs have become for text documents. The use of spreadsheets simplifies data entry, and allows results to be presented in a form that is immediately available for secondary analysis. Furthermore, since spreadsheets are a binary format, the results of numeric computations are available without loss of precision. When results are converted to text format, they are inevitably truncated in precision.

| | A | B | C | D | E | F | G | H |
|----|-----------------------------------|--------------|------|------|---|---|---|---|
| 1 | prof | case1 | | | | | | |
| 2 | Kc Distribution parameters | | | | | | | |
| 3 | muk | 29.4 | | | | | | |
| 4 | sigmak | 2.2 | | | | | | |
| 5 | Cumulative POD parameters | | | | | | | |
| 6 | mu | 0.05 | | | | | | |
| 7 | sigma | 0.5 | | | | | | |
| 8 | a_min | 0 | | | | | | |
| 9 | Peak load parameters | | | | | | | |
| 10 | asig | 1.26 | | | | | | |
| 11 | bsig | 21.7 | | | | | | |
| 12 | Aircraft parameters | | | | | | | |
| 13 | locs | 6 | | | | | | |
| 14 | acf | 125 | | | | | | |
| 15 | hpf | 1 | | | | | | |
| 16 | Data files | | | | | | | |
| 17 | avsf | crcksize.dat | | | | | | |
| 18 | avstime | a_vs_t.dat | | | | | | |
| 19 | abeta | geo.dat | | | | | | |
| 20 | repair | unif50.dat | | | | | | |
| 21 | avsr | | | | | | | |
| 22 | Usage Intervals | | | | | | | |
| 23 | usage | 1100 | 1100 | 1100 | | | | |

Figure 32. Example of a PROF Input Worksheet

PROFv2 controls Excel through a method called the Component Object Model (COM) that is the main part of what used to be called OLE (Object Linking and Embedding), but now seems to be called ActiveX. COM was invented to provide a standard way for Windows program modules to communicate with one another.

5.3 Probability of Fracture

Fracture occurs when an applied stress produces a stress intensity that exceeds the fracture toughness for the cracked detail, that is, when $\sigma \geq \sigma_c$. The probability of fracture (POF) can be expressed as

$$\text{POF} = \int_0^{a_c} f(a) \text{POF}(a) da + [1 - F(a_c)] \quad (7)$$

where $\text{POF}(a)$ is the probability of fracture for a specified crack size and a_c is the critical crack size. The basic mathematics underlying the calculation of the POF is unchanged from earlier versions of PROF. However, the identification of the function $\text{POF}(a)$, which is independent of the crack size distribution, is new. Also, a menu choice was added to calculate and plot $\text{POF}(a)$ versus crack size a .

Several improvements were made to the numerical methods used to calculate the probability of fracture. Although the adaptive integration routine used in PROF usually converges to the correct answer, in some cases the integration did not properly sample the tail of the distribution. This effect was corrected by partitioning the integral at the tabulated values of the crack size distribution table.

In previous versions of the PROF, the crack-size distribution was aged according to the crack growth curve for each time step, and a new extrapolation was fit to the tail of the aged crack-size distribution. In PROFv2, the integral in Equation 7 is calculated using the time 0 crack size distribution for each time step. The time effect is incorporated by using the aged crack length a^* in calculating the $\text{POF}(a)$ portion of the integrand of Equation 7. The effect of this change is to make the calculation of POF more robust by eliminating changes in the upper tail of the crack size distribution caused by numerically “growing” the cracks. In benign cases, there is no numerical difference in the results obtained. In more pathological cases, the results produced by the new method provided more reasonable answers than those generated by the old method.

The details of the probability of fracture (POF) may be found in Appendix B.

5.4 Residual Strength Function Input

PROFv2 was modified to allow optional use of a residual strength function $\sigma_R(a)$ in place of the geometry dependent function K/σ of crack size. As shown in Appendix B and described in Section 3.2, the residual strength curve eliminates an integral across the fracture toughness distribution. PROFv2 allows the residual strength function to be specified as a table of values.

5.5 Multi-Run Data Management

The multi-run analysis capability, described in Section 4, was added in PROFv2 by the introduction of the Excel interface. Problems with multiple variations can be expressed in one worksheet, as shown in Fig. 33. Each column is a separate case. In this example, there are two cases. During analysis, the results of each case are written on separate worksheets. A summary worksheet is also generated, as shown in Fig. 34. Specific analyses that combine the results of multiple cases can then be performed using Excel, as shown in Section 4.

The screenshot shows a Microsoft Excel window titled "Microsoft Excel - S7sedf.xls". The worksheet contains a table with two columns for "case1" and "case2". The rows are organized into sections: "Kc Distribution parameters", "Cumulative POD parameters", "Peak load parameters", "Aircraft parameters", "Data files", and "Usage Intervals".

| | A | B | C | D | E |
|----|-----------------------------------|--------------|--------------|---|---|
| 1 | prof | case1 | case2 | | |
| 2 | Kc Distribution parameters | | | | |
| 3 | muk | 51 | 51 | | |
| 4 | sigmak | 0.01 | 0.01 | | |
| 5 | Cumulative POD parameters | | | | |
| 6 | mu | 0.05 | 0.05 | | |
| 7 | sigma | 0.54 | 0.54 | | |
| 8 | a_min | 0 | 0 | | |
| 9 | Peak load parameters | | | | |
| 10 | asig | 4.088 | 4.088 | | |
| 11 | bsig | 5.0004 | 5.0004 | | |
| 12 | Aircraft parameters | | | | |
| 13 | locs | 1 | 1 | | |
| 14 | acf | 1 | 1 | | |
| 15 | hpf | 7.5 | 7.5 | | |
| 16 | Data files | | | | |
| 17 | avsf | s7ecs.dat | s7ecs.dat | | |
| 18 | avstime | s7a_vs_t.dat | s7a_vs_t.dat | | |
| 19 | repair | s7lnfit.dat | s7lnfit.dat | | |
| 20 | abeta | s7betas.dat | | | |
| 21 | avrs | | s7rs.dat | | |
| 22 | Usage Intervals | | | | |
| 23 | usage | 22500 | | | |

Fig. 33 Example of a Multi-Run Input Worksheet

Microsoft Excel - S7sedf.xls

File Edit View Insert Format Tools Data Window Help

Arial 10

| | A | B | C | D | E | F |
|----|-------|-------------|-------------|---|---|---|
| 1 | | case1 | case2 | | | |
| 2 | Hours | Prob of F | Prob of F | | | |
| 3 | 0 | 1.47135E-06 | 1.55681E-06 | | | |
| 4 | 2300 | 4.4109E-06 | 7.3367E-06 | | | |
| 5 | 4600 | 3.97875E-06 | 1.03384E-05 | | | |
| 6 | 6900 | 3.80578E-06 | 1.31479E-05 | | | |
| 7 | 9200 | 3.96391E-06 | 1.58533E-05 | | | |
| 8 | 11500 | 5.05855E-06 | 1.84983E-05 | | | |
| 9 | 13800 | 9.39352E-06 | 2.156E-05 | | | |
| 10 | 16100 | 6.76123E-05 | 7.61192E-05 | | | |
| 11 | 18400 | 0.02195052 | 0.021954535 | | | |
| 12 | 20700 | 0.034121271 | 0.034127173 | | | |
| 13 | 22500 | 0.043122569 | 0.043130167 | | | |
| 14 | | | | | | |

Ready

Figure 34. Example of a Multi-Run Output Worksheet.

Section 6

Summary and Recommendations

Probabilistically-based structural risk analyses are playing an increasingly important role in structural maintenance planning for aging aircraft. In particular, risk analysis is an additional tool that is being used in the determination of the maintenance intervals that ensure structural safety in fleets of aging aircraft. The stochastic risk analysis accounts for the variability in aging fleets that may not be covered by the conservative assumptions of deterministic damage tolerance analyses. The risk analysis computer program entitled Probability Of Fracture (PROF) is an aging aircraft risk analysis program that was originally designed to address the failure probabilities associated with a monolithic fatigue crack in a metal structural. (The Windows version of PROF is known as WinPROF). Although this code has been shown to be applicable to more general cracking scenarios, the use of PROF in these scenarios was, at best, awkward. Further, the original PROF/WinPROF was based on the Irwin fracture criterion and could not be used to evaluate failure risks in the event of discrete source damage. This report discusses the changes that were made to PROF/WinPROF to facilitate different risk analysis scenarios.

The changes made to update PROF/WinPROF fall into three categories:

- a) A new algorithm was added to calculate the conditional probability of failure given that an adjacent structure is in a failed state. This calculation is based on the criteria of the experienced stress exceeding residual strength where the residual strength is a function of crack size in the remaining structural component. A separate analysis to obtain the residual strength data would be necessary. An example is presented based on data and analysis of the fail-safe capability of a lower wing skin stringer in a Boeing 707 (JSTARS) airframe.
- b) An Excel Workbook interface was added to PROF to provide a data management capability for WFD scenarios that require multiple runs of PROF. The interface can be used to set up multiple analyses that can be performed in a single batch run of PROF. The output for each analysis is stored on a separate page of the workbook, along with a page that contains the conditional failure probabilities from each of the analyses. The Excel interface provides the macro and plotting capability to handle a

- broad range of WFD scenarios. Two examples are presented to demonstrate the application of multiple PROF runs to WFD scenarios: 1) analysis of specimens representative of C-135 lapjoints subjected to both MSD and corrosive thinning; and, 2) analysis of the multi-element damage problem from the C-141 Wing Station 405.
- c) In addition to the Excel interface, three other changes were made to WinPROF to enhance the Windows-PROF interface and to provide more stable calculations of fracture probabilities. The Windows interface has been changed from a third party user interface to Microsoft Foundation Classes. The FORTRAN programs that performed the analyses have been converted to C++. The changes in the computational algorithms remove some known idiosyncrasies that resulted from the method of handling the crack size distributions.

While the updated version of PROF is clearly superior to the original version, a number of potential enhancements were identified that were beyond the scope of the current program. It is recommended that PROF be further enhanced to:

- a) Access the Excel Workbook to obtain the PROF input that is currently obtained from ASCII files.
- b) Provide the capability to initiate analyses with a distribution of time to fixed crack size rather than a crack size distribution.
- c) Allow for a more general description of the maximum stress per flight distribution, possibly with a file format.
- d) Allow for a more general description of the inspection capability (POD) input, possibly with a file format.
- e) Add other failure mode criteria and necessary data provisions associated with the criteria.
- f) Interface PROF with a crack growth program.

In addition, PROF should be extensively exercised by performing a risk analysis for an entire airframe or major structural subsystem by combining results from all pertinent critical locations.

Section 7

References

1. Lincoln, J.W., "Risk Assessments – USAF Experience," Proceedings of the International Workshop on Structural Integrity of Aging Airplanes, Atlanta, GA, 31 March - 2 April 1992.
2. Berens, A.P., "Applications of Risk Analysis to Aging Military Aircraft," SAMPE Journal, Vol. 32, No. 5, September/October 1996, pp. 40-45.
3. Bell, R.P., Jones, K.M., and Alford, R.E., "Thoughts on Risk Analysis of an Aging Aircraft," WL-TR-97-4054, Proceedings of the 1996 USAF Aircraft Structural Integrity Program Conference, Volume 1, Wright Laboratory, Wright-Patterson Air Force Base, OH 45433, June 1997.
4. Berens, A.P., Hovey, P.W., and Skinn, D.A., "Risk Analysis for Aging Aircraft, Volume 1 – Analysis," WL-TR-91-3066, Air Force Research Laboratory, Wright-Patterson Air Force Base, Ohio, October, 1991.
5. Skinn, D.A., Berens, A.P., and Hovey, P.W., "Risk Analysis for Aging Aircraft Fleets, Volume II – User's Guide and Program Documentation," WL-TR-91-3068, Wright Laboratory, Wright-Patterson Air Force Base, Ohio, October 1991.
6. Papp, M.L. and Berens, A.P., "WINPROF Version 1.0, User's Guide," UDR-TR-95-69, University of Dayton, Dayton, Ohio, July, 1995.
7. Swift, T., "WFD Monitoring Issues and Concerns," presented at the 5th International Conference on Structural Airworthiness of New and Aging Aircraft, Hamburg Germany, 1993.
8. Schmidt, Hans-Juergen, *et. al.*, A Report of the Airworthiness Assurance Working Group, Final Report, Industry Committee on Widespread Fatigue Damage, July 1993.
9. Lincoln, John W., "Risk Assessments of Aging Aircraft," The First Joint DoD/FAA/NASA Conference on Aging Aircraft, J.P. Gallagher, Chairman, Ogden, Utah, July 1997.
10. Lincoln, John W., "Aging Aircraft – USAF Experiences and Actions," ICAF 97 – Fatigue in New and Aging Aircraft, R. Cook, P. Poole Eds., Proceedings of the 19th Symposium of the International Committee on Aeronautical Fatigue, Edinburgh Scotland, 18-20 June 1997.
11. The Boeing Company, Letter Reports and Spreadsheets submitted under Contract F34601-92-C-0272.
12. Scott, J.P., "Corrosion and Multiple Site Damage in Riveted Fuselage Lap Joints," Master's Thesis, Carleton University, March 1997.

13. Eastaugh, G.F., Simpson, D.L., Straznicky, P.V., and Wakeman, R.B., "A Special Uniaxial Coupon Test Specimen for the Simulation of Multiple Site Fatigue Crack Growth and Link-Up in Fuselage Skin Splices," National Research Council of Canada and Carleton University, AGARD-CP-568, December 1995.
14. D500-13008-1 (1998). "Corrosion Damage Assessment Framework", The Boeing Company, Seattle, WA. Release date August 5, 1998.
15. Trego, A., Cope, D., Johnson, P. and West, D, "Analytical Methodology for Assessing Corrosion and Fatigue in Fuselage Lap Joints," 1998 Air Force Corrosion Program Conference Proceedings, April 1998, Macon, Georgia.
16. Wawrzynek, P.A., and Ingraffea, A.R., "FRANC2D: A Two-Dimensional Crack Propagation Simulator, Version 2.7, User's Guide," NASA CR-4572, March 1994.
17. Swenson, D. and James, M., "FRANC2D/L: A Crack Propagation Simulator for Plane Layered Structures", Version 1.4 User's Guide, Kansas State University, December 1997.
18. Boyd, K., Harter, J.A., and Krishnan "AFGROW User's Manual Version 3.1.1," WL-TR-97-3053, Air Force Research Laboratory, Wright-Patterson Air Force Base, Ohio, February, 1998.
19. Berens, A.P., "Risk Analysis for C-141, WS405," UDR-TR-93-20, University of Dayton Research Institute, Dayton, OH, 45469-0120, January, 1993.
20. Cochran, J.B., Bell, R.P., Alford, R.E., and Hammond, D.O., "C-141 WS405 Risk Assessment," Proceedings of the 1991 USAF Structural Integrity Program Conference, San Antonio, Texas, December, 1991.

Appendix A

PROF Users Manual

This appendix describes how to use PROFv2. PROF and Microsoft Excel are used together. PROF data is stored in an Excel workbook on a worksheet named Input and PROF results are written to other Excel worksheets in the workbook.

A.1 PROF Installation

To install, copy PROF to any directory in the search path. PROF requires Microsoft Windows 95 (or later) and Excel 97 (part of Microsoft Office 97). PROF requires the following dynamic link libraries (DLL):

MFC42.DLL

MSVCRT.dll

KERNEL32.dll

USER32.dll

GDI32.dll

The last three should be on any system with Microsoft Windows. The first two need to be copied to C:\windows\system, if they are not already present. MFC42.DLL contains the Microsoft Foundation Classes. MSVCRT.DLL contains the Microsoft Visual C Run-time library routines.

A.2 Starting PROF

Start PROF by double-clicking on the PROF icon. A shortcut to the icon can be placed on your screen, if desired. When PROF activates, it first brings up a copy of Excel and opens a blank PROF input template. Do not close this copy of Excel while PROF is running.

A.3 PROF File Operations

The File menu in Windows contains menu items associated with opening and saving document files. It also contains a list of most recently used files, and a menu item that allows you to exit the application. The File menu for PROF is shown in Figure A-1:

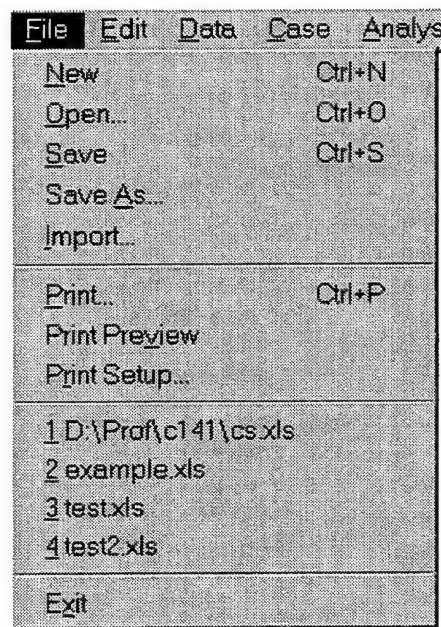


Figure A-1. PROF File Menu

A.3.1 Opening a New Input File

Start a new input file by selecting the File - New menu item. You will be prompted by a dialog box to save any currently-open modified spreadsheet. PROF will open a new blank input template sheet.

A.3.2 Opening Existing Input Files

PROF input files are stored as Excel spreadsheets, as shown in Figure A-2. You open an input file by selecting the File - Open menu item. This brings up the Windows common file selection dialog. Navigate to the directory containing the input spreadsheet and its associated data files, and select the desired spreadsheet.

| | A | B | C | D | E | F | G | H |
|----|-----------------------------------|--------------|------|------|---|---|---|---|
| 1 | prof | case1 | | | | | | |
| 2 | Kc Distribution parameters | | | | | | | |
| 3 | muk | 29.4 | | | | | | |
| 4 | sigmak | 2.2 | | | | | | |
| 5 | Cumulative POD parameters | | | | | | | |
| 6 | mu | 0.05 | | | | | | |
| 7 | sigma | 0.5 | | | | | | |
| 8 | a_min | 0 | | | | | | |
| 9 | Peak load parameters | | | | | | | |
| 10 | asig | 1.26 | | | | | | |
| 11 | bsig | 21.7 | | | | | | |
| 12 | Aircraft parameters | | | | | | | |
| 13 | locs | 6 | | | | | | |
| 14 | acf | 125 | | | | | | |
| 15 | hpf | 1 | | | | | | |
| 16 | Data files | | | | | | | |
| 17 | avsfa | crcksize.dat | | | | | | |
| 18 | avstime | a_vs_t.dat | | | | | | |
| 19 | abeta | geo.dat | | | | | | |
| 20 | repair | unif50.dat | | | | | | |
| 21 | avsr | | | | | | | |
| 22 | Usage Intervals | | | | | | | |
| 23 | usage | 1100 | 1100 | 1100 | | | | |

Figure A-2. Example of PROF Input Worksheet

A.3.3 Save and Save As Menu Items

The Save and Save As menu items operate in Excel.

A.3.4 Import Menu Item

Information from an input data file from the earlier version of PROF can be loaded in PROFv2. This is done using the File-Import menu item. Selecting this menu item activates a common file-open dialog box that allows you to enter the name of a file with the extension .ipt. This extension was used for earlier PROF input files. The input parameters replace the values in the current selected case.

A.3.5 Exiting PROF

The PROF application is exited by using the **File - Exit** menu item, by selecting the **Close** menu item (or using the **Ctrl-W** key) in the **System** menu, or by pressing the **Close** button at the far right side of the **Windows** menu.

As PROF prepares to close, PROF will prompt the user to save the Excel worksheet if it has been modified. PROF will also close the Excel application. It is not necessary or desirable for the user to close Excel directly. Closing Excel early can cause PROF to generate communication errors, since PROF expects that the Excel object it created is still active.

Closing Excel early can generate a variety of warning and error messages. If you inadvertently close Excel early, you should close PROF before doing any more work and then restart the PROF operation.

A.4 Modifying the Input Sheet

A valid PROF spreadsheet must contain a sheet called **Input**. An example of an input worksheet is shown in Figure A-2. The input sheet contains the input parameters. The first column of the input sheet consists of keywords and comments. The other columns of the spreadsheets contain different cases. Each case should be labeled by a short descriptive name on the top row (identified by the keyword `prof`). PROF examines this row and counts the number of consecutive non-blank columns to determine the total number of cases.

You can directly modify the input screen in Excel. If you make modifications to the input sheet this way, you must select the **Case - Reload** menu item. This causes PROF to reload the Excel input data.

You can also modify the input data from within PROF. The **Data** menu group contains menu items for this purpose.

A.5 Data

A.5.1 Files

PROF recognizes five types of numeric data files. Four of these are required before analysis can begin. The data files are:

1. Initial crack size cumulative distribution function ($F(a)$ vs. a).
2. Crack growth function (a vs. time).
3. Repaired crack cumulative distribution function.
4. Geometry factor (K/σ vs. a).
5. Residual strength (σ_{rs} vs. a).

Select the menu-item corresponding to desired type of data, Figure A-3

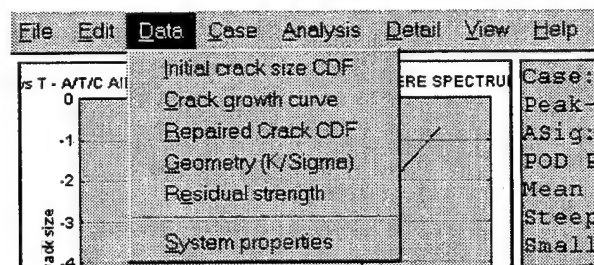
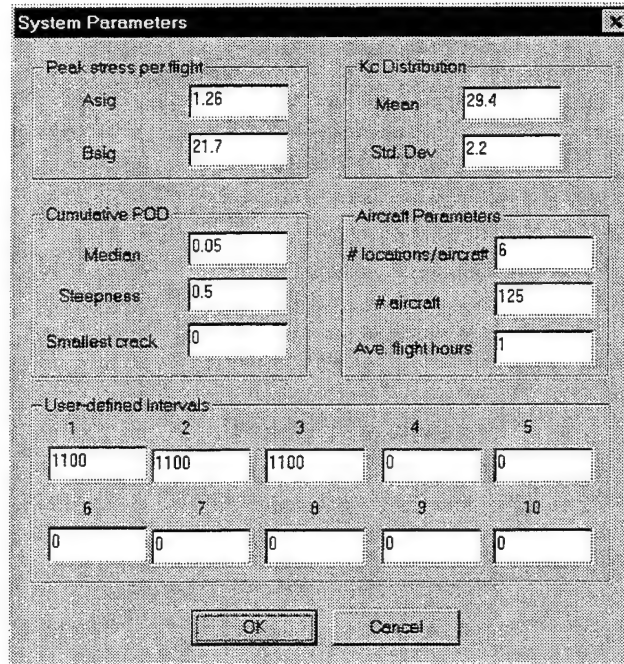


Figure A-3. PROF Data Menu

PROF will display a standard Windows File Open dialog box from which you may select the name of a data file.

A.5.2 System Properties

The Data - System Properties menu item, Figure A-4, activates the following dialog box:



System Parameters

| | | | | |
|------------------------|------|----------------------|------|----|
| Peak stress per flight | | Kc Distribution | | |
| Asig | 1.26 | Mean | 29.4 | |
| Bsig | 21.7 | Std. Dev | 2.2 | |
| Cumulative POD | | Aircraft Parameters | | |
| Median | 0.05 | # locations/aircraft | 6 | |
| Steepness | 0.5 | # aircraft | 125 | |
| Smallest crack | 0 | Ave. flight hours | 1 | |
| User-defined Intervals | | | | |
| 1 | 2 | 3 | 4 | 5 |
| 1100 | 1100 | 1100 | 0 | 0 |
| 6 | 7 | 8 | 9 | 10 |
| 0 | 0 | 0 | 0 | 0 |

OK Cancel

Figure A-4. PROF Data - System Properties Menu

The dialog allows the various numeric parameters for the current case to be changed.

A.6 Selecting a Case

Use the **Case - New** menu item to start a new case, Figure A-5, PROF will copy the parameters from the current case to the new column. Use the **Case - Select** menu item, Figure A-6, to change the current case. This activates a dialog box for the user to select the column in the input sheet from which to take input parameters.

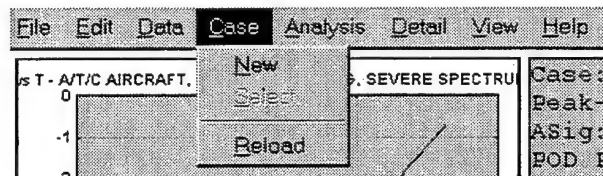


Figure A-5. PROF Case Menu

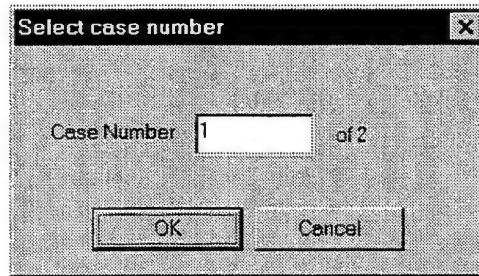


Figure A-6. PROF Case - Select Menu

The **Case - Reload** menu item reloads the information from the **Input** worksheet. Use **Reload** after you make any manual changes to the **Input** worksheet. PROF then scans the worksheet and updates the information for the currently selected case.

A.7 Analysis

The **Analysis** menu, Figure A-7, lists the execute code for analyzing all cases or a single case using the standard analysis (POF as a function of time) and POF(a) for the residual strength analysis.

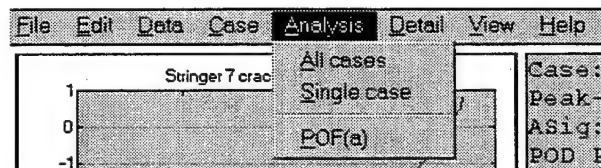


Figure A-7. PROF Analysis Menu

A.7.1 Standard Analysis Options

The **Analysis - Single case** menu item initiates an analysis for the current selected case. The PROF screen summarizes the results, as shown in Figure A-8. More details of the analysis are written to an Excel worksheet having the same name as the PROF case. An example of this output is shown in Figure A-9. The spreadsheet was reformatted by removing some blank columns and reduced in size to fit on the page. There are two separate groups of information. The group on the left tabulates the probability of failure at different times, and shows the expected effect of inspection and repair at the indicated intervals. The group on the right tabulates the crack size distribution at the start and end of each interval and before and after inspection/repair.

The rows below the crack-size distribution table in Fig. A-9 show the parameters λ and γ used to extrapolate the table. The extrapolation formula is

$$F_c(a) = 1 - \exp(-\lambda \cdot (a - \gamma)) \quad (A1)$$

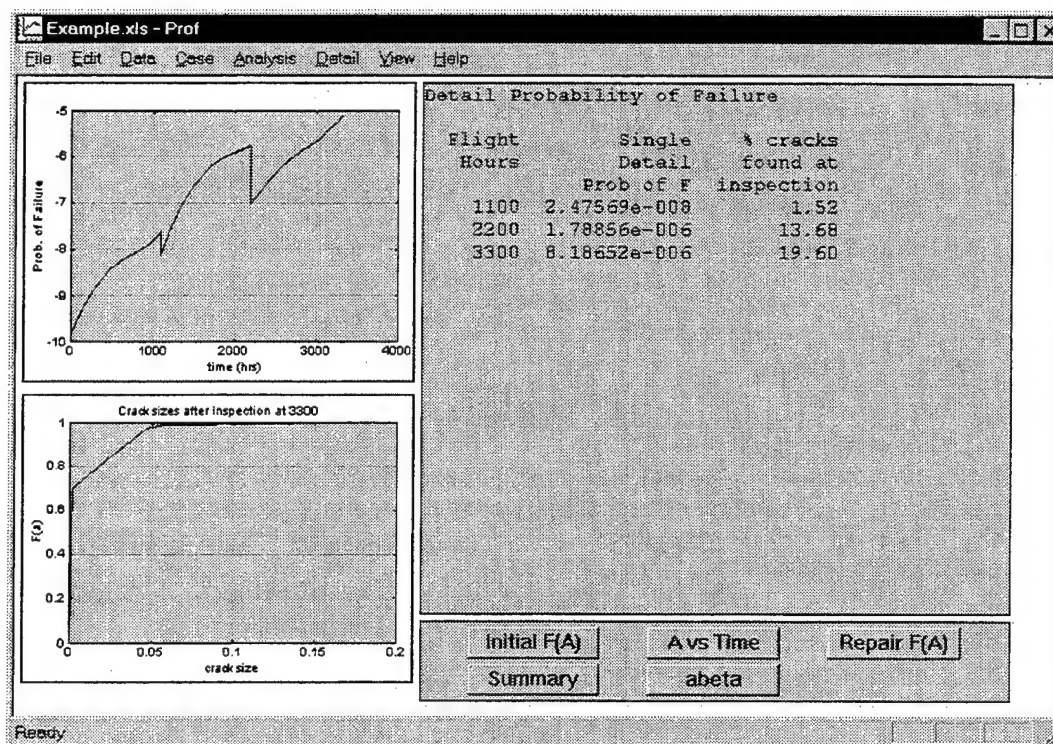


Figure A-8. Example Screen After a Single-Case Analysis

Microsoft Excel - test.xls

File Edit View Insert Format Tools Data Window Help

Font: Arial, 10, Bold, Italic, Underline, Text Color, Background Color, Font Color, Font Size, Font Style, Font Weight, Font Color, Font Size, Font Style, Font

Figure A-9. Example Worksheet for a Single-Case Analysis.
The Spreadsheet Was Reformatted to Fit this Page.

The Analysis - All Cases menu item performs a Single Case analysis for each case on the Input worksheet. This analysis results for each case appear in Excel as separate worksheets. The names of the worksheets are the same as the PROF case names assigned by the user on the Input worksheet. PROF also generates a worksheet named Results in which the probability of failure for each case is tabulated as a function of time. Figure A-10 contains an example of a results worksheet.

| | A | B | C | D | E | F |
|----|-------|-------------|-------------|---|---|---|
| 1 | | case1 | case2 | | | |
| 2 | Hours | Prob of F | Prob of F | | | |
| 3 | 0 | 1.47135E-06 | 1.55681E-06 | | | |
| 4 | 2300 | 4.4109E-06 | 7.3367E-06 | | | |
| 5 | 4600 | 3.97875E-06 | 1.03384E-05 | | | |
| 6 | 6900 | 3.80578E-06 | 1.31479E-05 | | | |
| 7 | 9200 | 3.96391E-06 | 1.58533E-05 | | | |
| 8 | 11500 | 5.05855E-06 | 1.84983E-05 | | | |
| 9 | 13800 | 9.39352E-06 | 2.156E-05 | | | |
| 10 | 16100 | 6.76123E-05 | 7.61192E-05 | | | |
| 11 | 18400 | 0.02195052 | 0.021954535 | | | |
| 12 | 20700 | 0.034121271 | 0.034127173 | | | |
| 13 | 22500 | 0.043122569 | 0.043130167 | | | |
| 14 | | | | | | |

Figure A-10. Example of Results Worksheet

A.7.2 Specialized Analysis Option

The Analysis - POF(a) menu item generates a plot and a table of the probability of failure as a function of crack size. Recall that the single-flight detail probability of failure P_f is calculated by PROF as

$$P_f = \int_0^{a_c} f(a) \text{POF}(a) da + [1 - F(a_c)] \quad (\text{A2})$$

where $f(a)$ is the crack-size distribution function, $F(a)$ is the cumulative distribution function, and a_c is the critical crack size.

Figure A-11 shows an example of the PROF screen after a calculation of $POF(a)$. A longer output table is also generated in an Excel worksheet called *pof*.

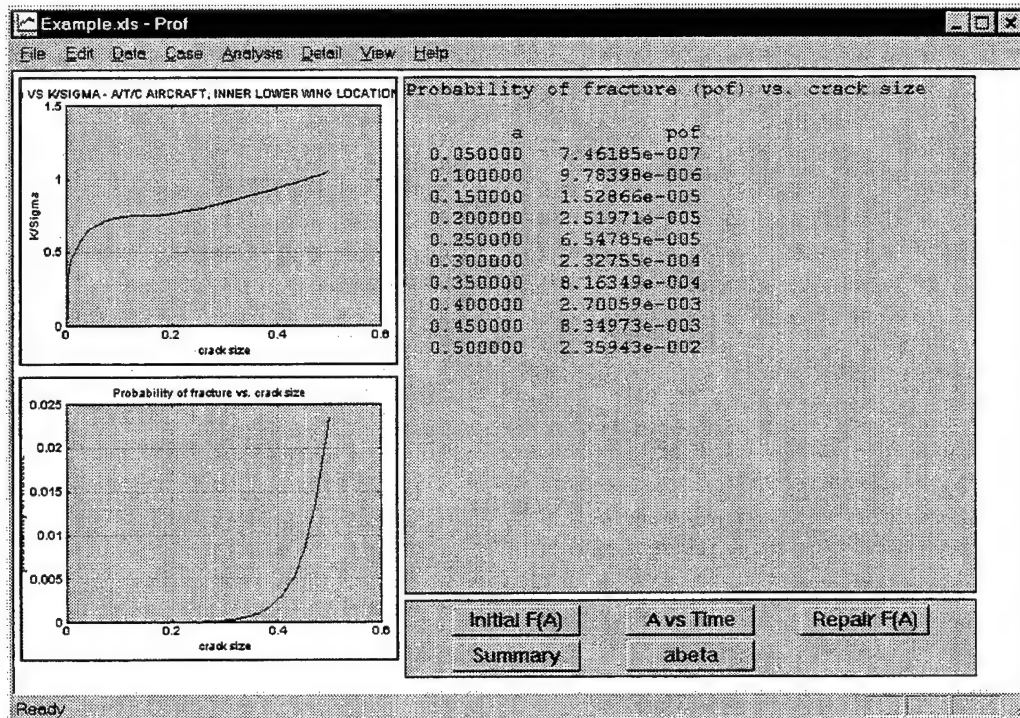


Figure A-11. Example Display for $POF(a)$

A.8 Detail Calculations

The Detail menu, Figure A-12, provides support for examining the detailed results of some of the analytic calculations. There are three menu items in this group:

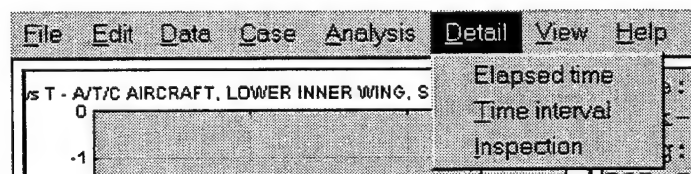


Figure A-12. PROF Detail Menu

Each menu item brings up a dialog box.

A.8.1 Elapsed Time

The Detail - Elapsed Time choice, Figure A-13, calculates the probability of failure at a selected time interval since inspection. This time interval is chosen in the dialog box shown below. This choice is a debugging tool which can be used to calculate probability of fracture at any selected time.

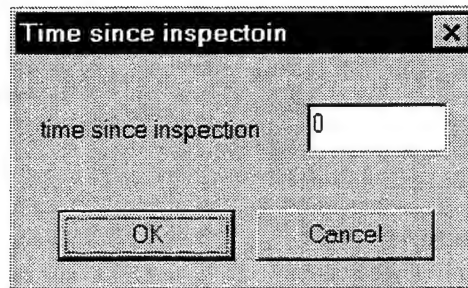


Figure A-13. PROF Detail - Time Since Inspection Menu

A cropped example of PROF screen output is shown in Figure A-14, for a time of 1100.

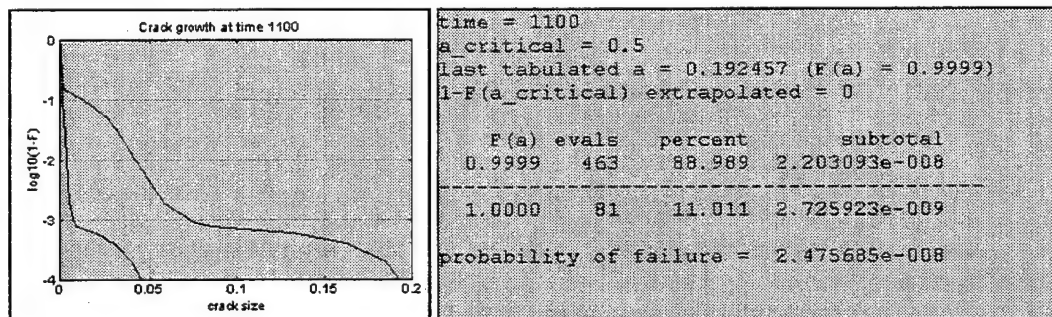


Figure A-14. Example Elapsed Time Calculation Screen

The left curve in the figure shows the starting crack size distribution, plotted as $\log_{10}(1-F)$ (exceedance) versus crack size. The right curve shows the expected crack size distribution at the specified time interval, calculated from the crack growth curve. The text window shows various terms in the POF calculation. The column labeled *evals* is the number of function evaluations of $POF(a)$ in the integral. This number is indicative of the rate of convergence of the numerical integration. The column labeled *percent* shows the contribution of each term to the total.

If the maximum crack size in the extended (growth) crack distribution table is less than the critical crack size, the POF is the sum of the following terms:

| | |
|---|--|
| Interpolated region | $\int_0^{a_n} f(a) \text{POF}(a) da$ |
| Extrapolated region | $\int_{a_n}^{a_c} f(a) \text{POF}(a) da$ |
| Extrapolated probability that crack exceeds critical size | $1 - F_c$ |

In these expressions, a_n is the last value in the crack distribution table and a_c is the critical crack size.

If the maximum crack size in the extended (growth) crack size distribution is greater than the critical crack size, F_c is interpolated rather than extrapolated, and the POF is the sum of the following terms:

| | |
|---|--------------------------------------|
| Interpolated region | $\int_0^{a_c} f(a) \text{POF}(a) da$ |
| Interpolated probability that crack exceeds critical size | $1 - F_c$ |

The dashed line in the text window divides the interpolated region of the crack size distribution from the extrapolated region. In the example of Figure A-14, the probability of cracks larger than the critical size is zero, or more precisely F_c is indistinguishable from unity in computer arithmetic (double precision floating-point numbers).

More details of this calculation are generated as a new sheet in Excel, as shown in Figure A-15. The columns on the left show region subtotals of the POF calculation. The rows where the probability is less than 10^{-15} are suppressed. The columns on the right show the tabulated crack distribution at the start and end of the specified interval.

| | A | B | C | D | E | F | G | H |
|----|--------------------------|-------|----------|----------|---|----------|----------|-------------|
| 1 | time | 1100 | | | | F | a before | a after |
| 2 | a_critical | | | 0.5 | | 0 | 0 | 0 |
| 3 | last tabulated a | | | 0.192457 | | 0.000101 | 0.000076 | 7.69904E-05 |
| 4 | 1-F(a_crit) extrapolated | | | 0 | | 0.001001 | 0.000114 | 0.000115486 |
| 5 | | | | | | 0.009993 | 0.000184 | 0.000186398 |
| 6 | probability of failure | | | 2.48E-08 | | 0.024979 | 0.000232 | 0.000235023 |
| 7 | | | | | | 0.049955 | 0.000283 | 0.000286688 |
| 8 | F(a) | evals | subtotal | total | | 0.099907 | 0.000356 | 0.000360639 |
| 9 | 0.899135 | 46 | 1.72E-13 | 1.72E-13 | | 0.149858 | 0.000416 | 0.000421421 |
| 10 | 0.949095 | 18 | 8.67E-11 | 8.69E-11 | | 0.199809 | 0.00047 | 0.000476125 |
| 11 | 0.97408 | 57 | 5.62E-10 | 6.49E-10 | | 0.299711 | 0.000575 | 0.000582493 |
| 12 | 0.989079 | 65 | 1.71E-09 | 2.36E-09 | | 0.499516 | 0.000799 | 0.000809412 |
| 13 | 0.998113 | 18 | 5.51E-09 | 7.87E-09 | | 0.699322 | 0.001112 | 0.001169899 |
| 14 | 0.999066 | 18 | 2.56E-09 | 1.04E-08 | | 0.799227 | 0.001359 | 0.001568199 |
| 15 | 0.9992 | 6 | 7.18E-10 | 1.12E-08 | | 0.84918 | 0.001536 | 0.003062509 |
| 16 | 0.9994 | 106 | 2.16E-09 | 1.33E-08 | | 0.899135 | 0.001793 | 0.013756096 |
| 17 | 0.9996 | 40 | 2.98E-09 | 1.63E-08 | | 0.949095 | 0.002255 | 0.027316649 |
| 18 | 0.9998 | 49 | 3.59E-09 | 1.99E-08 | | 0.97408 | 0.00275 | 0.03368184 |
| 19 | 0.9999 | 40 | 2.15E-09 | 2.2E-08 | | 0.989079 | 0.003465 | 0.041218778 |
| 20 | | | | | | 0.998113 | 0.005606 | 0.058595083 |
| 21 | 1 | 81 | 2.73E-09 | 2.48E-08 | | 0.999066 | 0.00833 | 0.076099515 |
| 22 | | | | | | 0.9992 | 0.01 | 0.086679515 |
| 23 | | | | | | 0.9994 | 0.02 | 0.131436588 |
| 24 | | | | | | 0.9996 | 0.03 | 0.162185995 |
| 25 | | | | | | 0.9998 | 0.04 | 0.185004891 |
| 26 | | | | | | 0.9999 | 0.045 | 0.192456625 |

Figure A-15. Example of Detail - Elapsed Time Spreadsheet

A.8.2 Time Interval

The Detail - Time Interval menu choice, Figure A-16, calculates the probability of failure over an interval starting at a specified time. The associated dialog box is shown below:

| Time interval | |
|---|------|
| Starting time | 0 |
| Evaluation interval | 1100 |
| Number of points | 10 |
| <input type="button" value="OK"/> <input type="button" value="Cancel"/> | |

Figure A-16. PROF Detail - Time Interval Menu

The first edit box is the time since inspection at which to begin calculations. The evaluation interval is the time interval after the start of calculations. If the time since inspection is 800, and the evaluation interval is 1000, then the last time for which a calculation is made is 1800. The evaluation interval is divided into 10 divisions. A typical screen display is shown in Figure A-17:

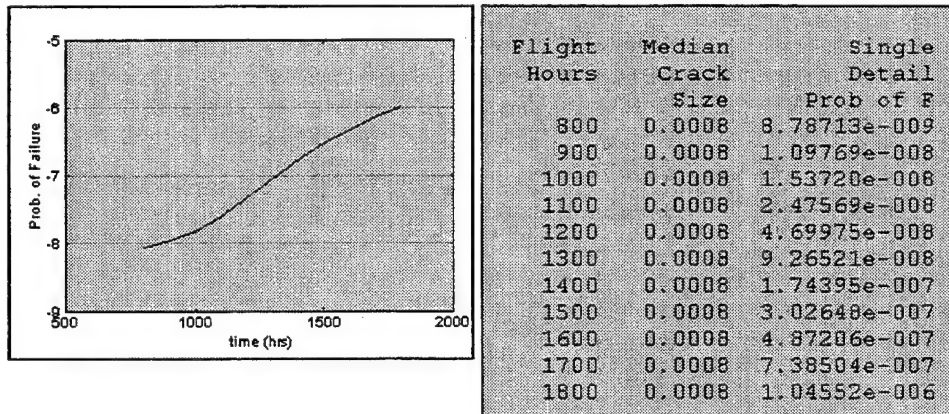


Figure A-17. Example Time Interval Calculation Screen

The example worksheet in Figure A-18 shows the median crack size and probability of failure at each time in the interval. Also shown is the relative contribution of the exceedance probability for cracks growing to above the critical size relative to the total probability of failure.

| | A | B | C | D |
|----|--------------|-------------------|-------------------------|--------------------------------------|
| | Flight Hours | Median Crack Size | Single Detail Prob of F | Ratio of (1-F_critical) to Prob of F |
| 4 | 800 | 0.000807398 | 1.96535E-08 | 0 |
| 5 | 900 | 0.000808361 | 2.48437E-08 | 0 |
| 6 | 1000 | 0.000809322 | 3.57357E-08 | 0 |
| 7 | 1100 | 0.000810286 | 5.93469E-08 | 0 |
| 8 | 1200 | 0.00081125 | 1.14339E-07 | 0 |
| 9 | 1300 | 0.000812216 | 2.24202E-07 | 1.0399E-08 |
| 10 | 1400 | 0.000813183 | 4.14102E-07 | 9.5445E-08 |
| 11 | 1500 | 0.000814151 | 7.02205E-07 | 1.20049E-06 |
| 12 | 1600 | 0.000815123 | 1.10396E-06 | 1.25689E-05 |
| 13 | 1700 | 0.000816094 | 1.63935E-06 | 4.65902E-05 |
| 14 | 1800 | 0.000817071 | 2.26525E-06 | 0.001101904 |

Figure A-18. Example Worksheet Created by Selecting Detail - Time Interval

A.8.3 Inspection

The Detail - Inspection menu item, Figure A-19, calculates the before-inspection and after-inspection crack size distributions at a selected time. The associated dialog box is:

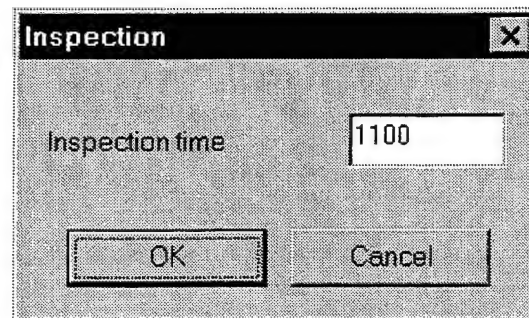


Figure A-19. PROF Detail - Inspection Menu

An example of the screen display is shown in Figure A-20:

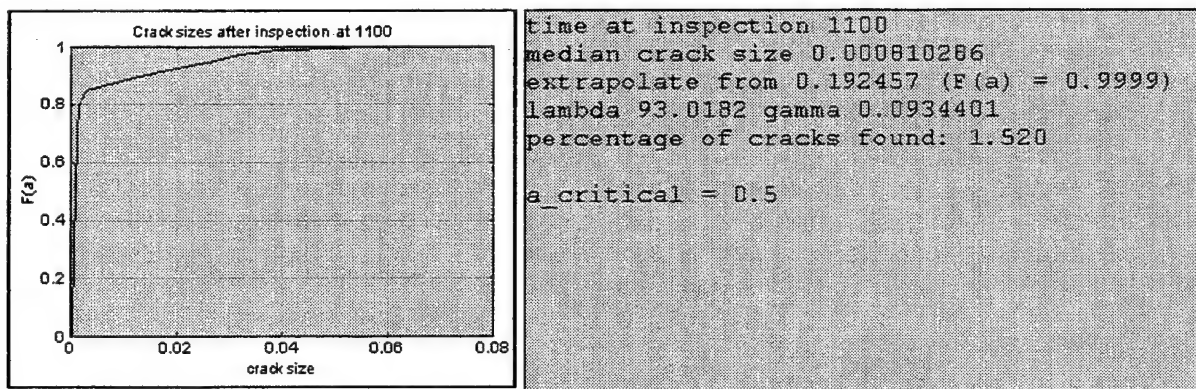


Figure A-20. Example Inspection Calculation Screen

The crack-size distribution after inspection is shown on the left. Some information about the tabulated distribution function is shown on the right.

An Excel worksheet is also generated, as shown in Figure A-21. The columns tabulated the distribution of cracks at the start of the interval, at the end of the interval (just before inspection), and just after inspection.

| | A | B | C | D | E |
|----|----------|----------|----------|----------|---|
| 1 | time | 0 | 1100 | 1100 | |
| 2 | | start | before | after | |
| 3 | fa | a | a | a | |
| 4 | 0 | 0 | 0 | 0 | 0 |
| 5 | 0.000101 | 0.000076 | 7.7E-05 | 6.25E-05 | |
| 6 | 0.001001 | 0.000114 | 0.000115 | 0.000114 | |
| 7 | 0.009993 | 0.000184 | 0.000186 | 0.000186 | |
| 8 | 0.024979 | 0.000232 | 0.000235 | 0.000235 | |
| 9 | 0.049955 | 0.000283 | 0.000287 | 0.000287 | |
| 10 | 0.099907 | 0.000356 | 0.000361 | 0.00036 | |
| 11 | 0.149858 | 0.000416 | 0.000421 | 0.000421 | |
| 12 | 0.199809 | 0.00047 | 0.000476 | 0.000476 | |
| 13 | 0.299711 | 0.000575 | 0.000582 | 0.000582 | |
| 14 | 0.499516 | 0.000799 | 0.000809 | 0.000809 | |
| 15 | 0.699322 | 0.001112 | 0.00117 | 0.001169 | |
| 16 | 0.799227 | 0.001359 | 0.001568 | 0.001566 | |
| 17 | 0.84918 | 0.001536 | 0.003063 | 0.003035 | |
| 18 | 0.899135 | 0.001793 | 0.013756 | 0.01294 | |
| 19 | 0.949095 | 0.002255 | 0.027317 | 0.025752 | |
| 20 | 0.97408 | 0.00275 | 0.033682 | 0.032056 | |
| 21 | 0.989079 | 0.003465 | 0.041219 | 0.039167 | |
| 22 | 0.998113 | 0.005606 | 0.058595 | 0.051246 | |
| 23 | 0.999066 | 0.00833 | 0.0761 | 0.054044 | |
| 24 | 0.9992 | 0.01 | 0.08668 | 0.05466 | |
| 25 | 0.9994 | 0.02 | 0.131437 | 0.055804 | |
| 26 | 0.9996 | 0.03 | 0.162186 | 0.057416 | |
| 27 | 0.9998 | 0.04 | 0.185005 | 0.062089 | |
| 28 | 0.9999 | 0.045 | 0.192457 | 0.068192 | |
| 29 | | | | | |

Figure A-21. Example of Spreadsheet Generated by the Detail - Inspection Menu Item

A.9 Viewing Data Files

The View menu group, Figure A-22, is used to cycle through displays of the PROF input data files.

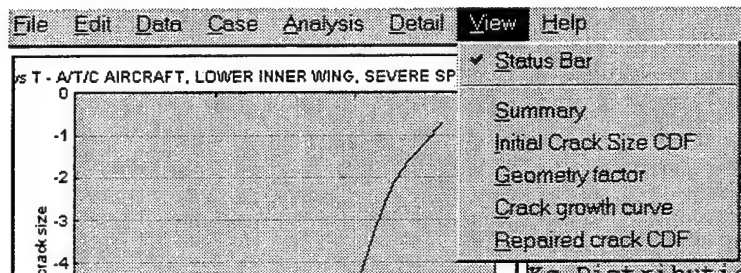


Figure A-22. PROF View Menu

The buttons in the group on the bottom right of the PROF window, Figure A-23, perform the same function.

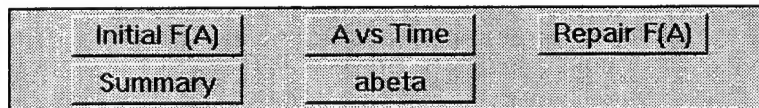
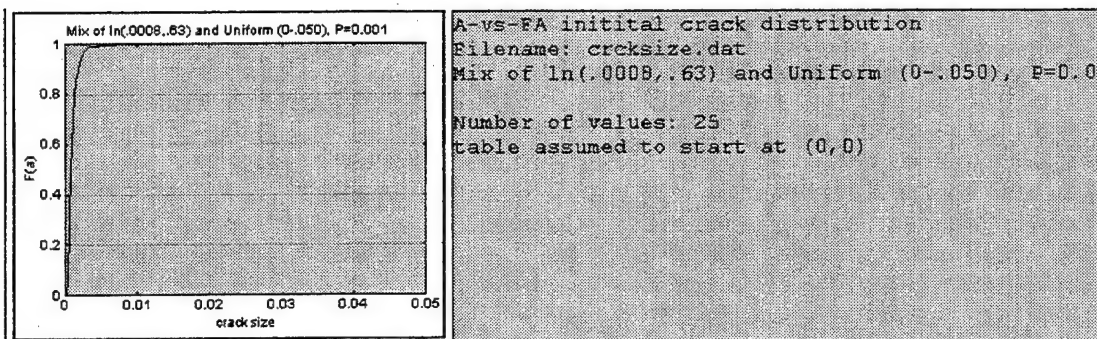


Figure A-23. PROF Screen Buttons

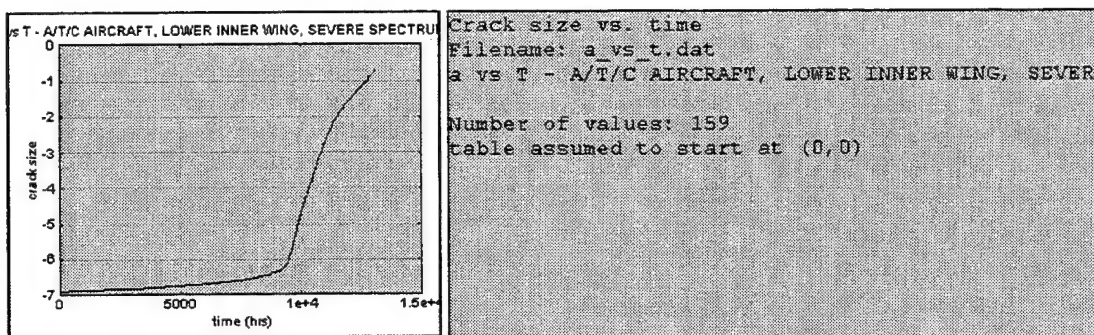
The Summary button (or menu choice) generates an overall summary of the input parameters.

Figure A-24 shows some examples of the display of different data files. The text window displays the general description of the data file. The first line is a basic description of the type of data file. The next line shows the filename. The third line displays the specific description of the data stored in the first line of the data file. The following lines show the number of values tabulated and other messages about the data file, such as whether the table is assumed to start at (0, 0).

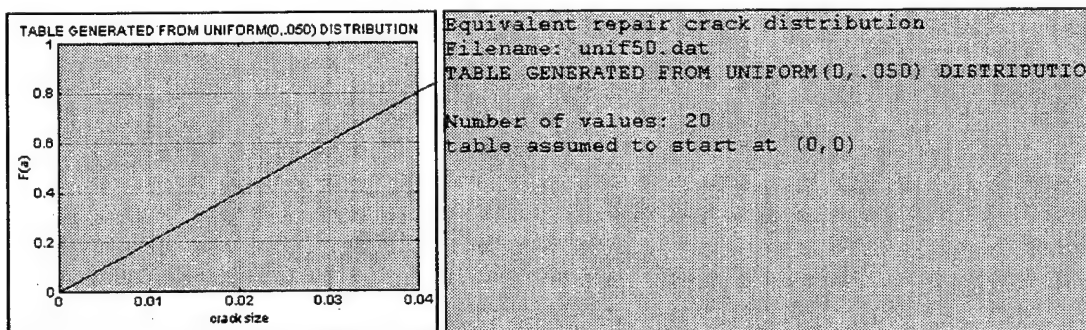
Buttons are shown only after a filename is specified for each type of data file. The summary button does not appear until all data files have been specified.



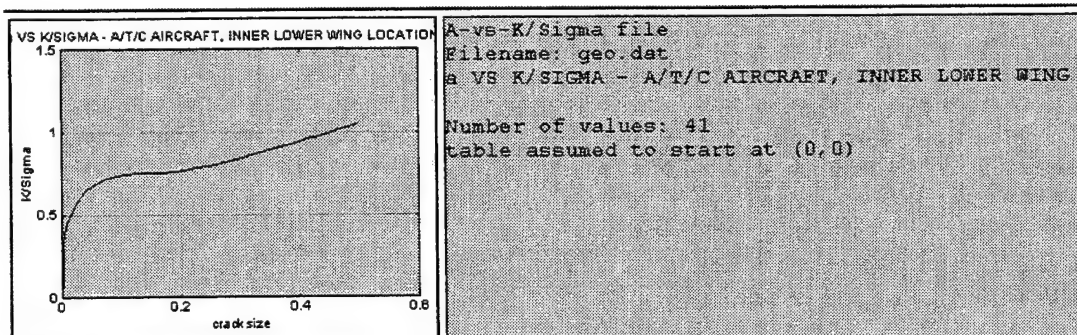
(a) Example of initial crack distribution data



(b) Example of crack growth data



(c) Example of equivalent repair crack distribution data



(d) Example of geometry data file

Figure A-24. Sample View Output for Different Data Files

Appendix B

Numerical Methods in PROF

This appendix documents the numerical methods used in PROF and discusses some of the tests that were used to validate the calculations.

B.1 Probability of Fracture

Fracture occurs when an applied stress produces a stress intensity that exceeds the fracture toughness for the cracked detail, that is, when

$$\sigma \geq \sigma_c = \frac{K_c}{\sqrt{\pi a} \beta(a)} \quad (\text{B1})$$

where a is the crack size, K_c is the fracture toughness of the material and $\beta(a)$ is a geometry dependent factor. The probability of fracture (POF) is calculated as

$$\text{POF} = P\{\sigma_{\max} \geq \sigma_{cr}\} \quad (\text{B2})$$

The defining relationship between stress intensity factor, stress, and crack size is expressed as

$$\frac{K}{\sigma} = \sqrt{\pi a} \beta(a) \quad (\text{B3})$$

PROF obtains K/σ versus a as an input table.

The probability of fracture (POF) calculation is performed through a double integral across crack size and fracture toughness

$$\text{POF} = \int_0^{a_c} f(a) \int_0^{\infty} g(K_c) \hat{H}(\sigma_c(a, K_c)) dK_c da + [1 - F(a_c)] \quad (\text{B4})$$

where $f(a)$ is the crack-size probability density function, $g(K_c)$ is the fracture-toughness probability density function, $\hat{H}(\sigma) = 1 - H(\sigma)$ is the exceedance probability distribution function for the peak stress in a single flight, and $\sigma_c(a, K_c)$ is the critical stress for the given crack size and fracture toughness.

A normal probability density function is used to model $g(K_c)$

$$g(x) = \text{dnorm}(x, \mu, \sigma) = \frac{1}{\sigma\sqrt{2\pi}} \exp\left(-\frac{(x-\mu)^2}{2\sigma^2}\right) \quad (\text{B5})$$

Gumbel type 1 distribution is used to model the distribution of the maximum stress per flight and is given by

$$P\{\sigma_{\max} \geq \sigma\} = \hat{H}(\sigma) = 1 - \exp\left(-\exp\left(-\frac{\sigma - B}{A}\right)\right) \quad (\text{B6})$$

where A and B are parameters that must be supplied by the user.

The probability of fracture can be simplified to

$$\text{POF} = \int_0^{a_c} f(a) \text{POF}(a) da + [1 - F(a_c)] \quad (\text{B7})$$

where $\text{POF}(a)$ is the probability of fracture for a specified crack size, given by

$$\text{POF}(a) = \int_0^{\infty} g(K_c) \hat{H}(\sigma_c(a, K_c)) dK_c \quad (\text{B8})$$

In the case of residual-strength data, the probability of fracture as a function of crack size is given by

$$\text{POF}(a) = \hat{H}(\sigma_r(a)) \quad (\text{B9})$$

where $\sigma_r(a)$ is the residual strength of the cracked detail as a function of crack size.

Equation B7 is the analytical formula for determining POF. However, the numerical evaluation of Equation B7 is susceptible to inaccuracies because $f(a)$ must be determined from a table of values of the cumulative distribution function $F(a)$ rather than from an explicit mathematical formula. A better numerical approach is to apply a change of variables that will use $F(a)$ rather than $f(a)$. This is accomplished by using the fact that if u is a uniform random variable on the interval $(0, 1)$ then $x = F^{-1}(u)$ has the distribution function $F(x)$. Equation B-7 can then be written as

$$\text{POF} = \int_0^{a_c} \text{POF}(F^{-1}(u)) du + [1 - F(a_c)] \quad (\text{B10})$$

This version of Equation B-7 eliminates the need to use the inaccurate numerical determination of $f(a)$ from $F(a)$.

B.2 Calculating Probability of Failure versus Crack Size

PROF calculates the probability of failure $POF(a)$ using a Gauss-Hermite integration method. Gauss-Hermite quadrature was developed for integrals involving the normal probability density function.

PROFv2 allows this function to be calculated and plotted directly. This allows us to compare the results with those obtained by analytic methods.

For example, the following model for K/σ was used to generate a table of input values for PROF and in analytic calculations

$$\frac{K}{\sigma} = \sqrt{\pi a} \beta(a) = \frac{\sqrt{\pi a} \sec(\pi a/2)}{1.5 - 1.1708 \exp(-4.914a)} \quad (B11)$$

The difference between these two methods is that PROF uses interpolation to find intermediate input values for K/σ , whereas an analytic calculation uses a formula to find intermediate values. In both cases, numerical integration techniques are employed. However, the numerical methods used by the mathematical software (MathCAD, for the validation calculations in this instance) may be different than those used by PROF. Note that the method used by the mathematical software package is not necessarily superior to that used by PROF. A better check involves incorporating the analytic expression into PROF, so that the comparison is based solely on the integration technique.

B.3 Probability of Failure During Flight

The current version of PROF calculates a single-flight detail probability of failure as the sum of the probability of fracture during the current flight plus the probability that the crack size exceeds the critical crack size a_c just prior to the flight.

$$P_f = \int_0^{a_c} f(a) \text{POF}(a) da + [1 - F(a_c)] \quad (\text{B12})$$

If the maximum crack size in the extended (growth) crack distribution table is less than the critical crack size, the probability of failure is the sum of the following terms:

| | |
|---|---|
| Interpolated region | $\int_0^{F_n} \text{POF}(F^{-1}(u)) du$ |
| Extrapolated region | $\int_{F_n}^{F_c} \text{POF}(F^{-1}(u)) du$ |
| Extrapolated probability that crack exceeds critical size | $1 - F_c$ |

where F_n is the last value in the crack distribution table and F_c is the extrapolated value of the cumulative crack distribution function at the critical crack size.

If the maximum crack size in the extended (growth) crack size distribution table is greater than the critical crack size, F_c is interpolated rather than extrapolated, and the POF is the sum of the following terms:

| | |
|---|---|
| Interpolated region | $\int_0^{F_c} \text{POF}(F^{-1}(u)) du$ |
| Interpolated probability that crack exceeds critical size | $1 - F_c$ |

PROF uses the following function to extrapolate beyond the last tabulated value F_n of the crack-size distribution table:

$$F_e(a) = 1 - \exp(-\lambda(a - \gamma)) \quad (\text{B13})$$

This function is linear in a plot of the log exceedance probability, $\log(1 - F(a))$ versus crack length.

The calculation of the probability of fracture is performed incrementally, using the crack-size distribution function $F(a)$, as

$$\text{POF}_i = \int_{F_{i-1}}^{F_i} \text{POF}(F^{-1}(u)) du \quad (\text{B14})$$

using an adaptive Rhomberg quadrature method. A final step calculates the value from F_n to F_c where $F_c = F^{-1}(a_c)$ and F_n is the value in the table less than F_c .

B.4 Verification of Calculations

This section describes some tests to verify the calculations performed by PROF, by comparing the results to those obtained by the numerical methods in MathCAD. The assumed log-normal distribution function does not have linear behavior near the extrapolation region. To compare PROF results with those calculated using MathCAD, we must force PROF to avoid extrapolation. In the new version of PROF this can be done by continuing the tabulated distribution to the critical crack-size a_c , because the new version uses this table as provided. The previous version of PROF resampled the input distribution prior to making calculations. This resampling effectly truncated the distribution table and reintroduced extrapolation.

B.4.1 Example 1

The first example is based on a median crack size $\mu = 0.0008$.

Table B-1 shows a table of the incremental contributions to the probability of fracture. PROF skips the Rhomberg quadrature when $\text{POF}(a)$ at the end of the increment is less than 10^{-15} . Notice how large $F(a)$ is before there is a contribution to the probability of fracture. This point corresponds to a crack size of about 0.01. The number of evals is a count of function evaluations for the Rhomberg integration.

Table B-1. Example 1: Details of the Calculation of the Probability of Failure

| F(a) | evals | subtotal | total |
|--|-------|---------------|---------------|
| 0.990000000000 | 42 | 6.203554e-018 | 6.203554e-018 |
| 0.992000000000 | 18 | 1.530229e-016 | 1.592265e-016 |
| 0.994000000000 | 18 | 7.736282e-015 | 7.895509e-015 |
| 0.996000000000 | 77 | 1.527556e-013 | 1.606511e-013 |
| 0.998000000000 | 18 | 8.723695e-013 | 1.033021e-012 |
| 0.999000000000 | 18 | 3.870302e-012 | 4.903323e-012 |
| 0.999200000000 | 6 | 3.132779e-012 | 8.036102e-012 |
| 0.999400000000 | 58 | 6.581122e-012 | 1.461722e-011 |
| 0.999600000000 | 6 | 1.181790e-011 | 2.643512e-011 |
| 0.999800000000 | 10 | 3.018542e-011 | 5.662054e-011 |
| 0.999900000000 | 10 | 4.169218e-011 | 9.831273e-011 |
| 0.999996097620 | 113 | 1.582158e-010 | 2.565286e-010 |
| 0.999999840728 | 38 | 2.894822e-011 | 2.854768e-010 |
| 0.999999979613 | 26 | 7.591650e-012 | 2.930684e-010 |
| 0.999999995636 | 26 | 9.931910e-012 | 3.030003e-010 |
| 0.999999998741 | 18 | 2.637277e-011 | 3.293731e-010 |
| 1.000000000000 | | 1.259000e-009 | 1.588373e-009 |
| probability of failure = 1.588373e-009 | | | |

PROF generates a short summary of these results, Table B-2:

Table B-2. Example 1: Summary of Results

| F(a) | evals | percent | subtotal |
|--|-------|---------|---------------|
| 1.00000 | 502 | 20.737 | 3.293731e-010 |
| 1.00000 | | 79.263 | 1.259000e-009 |
| probability of failure = 1.588373e-009 | | | |

The first row is the probability of fracture (with an associated evaluation count). The second row is the probability that a_c was exceeded at the start of the flight. The percent column shows the total contribution of each term to the final probability of failure.

The final probability corresponds to that obtained with a MathCAD calculation. To illustrate the importance of the tail region in this example, we truncated the initial crack distribution table at $F(a)$ of 0.9999 (corresponding to $a = 0.0444$). The difference in the resulting calculation, Table B-3, can be attributed to extrapolation error for a log-normal model.

Table B-3. Example 1: Comparison of Failure Probabilities for Crack Size Distribution Extrapolation

| Description | Calculated Probability of Failure |
|--|-----------------------------------|
| Crack size distribution table extended to $a = 0.5$ | 1.58837e-09 |
| Crack size distribution table truncated at $F(a)=0.9999$ | 2.36851e-10 |

This exercise demonstrates the effect of the tail region on the final results. Note that although the absolute results are sensitive to the assumptions made about the tail region, the relative results obtained in parametric studies may be less sensitive to the behavior in the tail region. In any case, the extrapolation method used by PROF may be avoided by extending the tabulated distribution function to larger crack sizes.

B.4.2 Example 2

The second example is based on a median crack size of 0.005 and represents a hypothetical growth of an initial crack distribution (example 1) over a time of 3800 hours.

A summary of the results is shown in Table B-4. A detailed table of results is shown in Table B-5.

Table B-4. Example 2: Summary of Results

| F(a) | evals | percent | subtotal |
|--|-------|---------|---------------|
| 1.00000 | 557 | 2.384 | 2.452650e-007 |
| 1.00000 | | 97.616 | 1.004474e-005 |
| probability of failure = 1.029000e-005 | | | |

Figure B-5. Example 2: Details of the Calculation of the Probability of Failure

| F(a) evals | | subtotal | total |
|--|----|---------------|---------------|
| 0.80000 | 34 | 4.256965e-013 | 4.256965e-013 |
| 0.85000 | 94 | 7.130495e-012 | 7.556192e-012 |
| 0.90000 | 10 | 6.201949e-011 | 6.957568e-011 |
| 0.95000 | 65 | 1.557306e-009 | 1.626881e-009 |
| 0.97500 | 75 | 5.581802e-009 | 7.208683e-009 |
| 0.98000 | 6 | 2.858829e-009 | 1.006751e-008 |
| 0.99000 | 10 | 1.167660e-008 | 2.174411e-008 |
| 0.99200 | 49 | 4.015875e-009 | 2.575999e-008 |
| 0.99400 | 28 | 5.014769e-009 | 3.077476e-008 |
| 0.99600 | 6 | 6.530056e-009 | 3.730481e-008 |
| 0.99800 | 40 | 9.221079e-009 | 4.652589e-008 |
| 0.99900 | 10 | 6.986390e-009 | 5.351228e-008 |
| 0.99920 | 44 | 1.901435e-009 | 5.541372e-008 |
| 0.99940 | 10 | 2.296068e-009 | 5.770979e-008 |
| 0.99960 | 10 | 3.066090e-009 | 6.077588e-008 |
| 0.99980 | 10 | 5.356070e-009 | 6.613195e-008 |
| 0.99990 | 10 | 6.729175e-009 | 7.286112e-008 |
| 0.99992 | 10 | 3.743473e-009 | 7.660459e-008 |
| 0.99998 | 18 | 3.398123e-008 | 1.105858e-007 |
| 0.99999 | 18 | 1.346792e-007 | 2.452650e-007 |
| 1.00000 | | 1.004474e-005 | 1.029000e-005 |
| probability of failure = 1.029000e-005 | | | |

The probability of failure was calculated four different ways, as shown in Table B-6.

**Table B-6. Example 2: Comparison of Failure Probabilities
for Crack Size Distribution in Extrapolations**

| | Distribution extended to $a = a_c$ | Distribution truncated at 0.9999 |
|--|---------------------------------------|-------------------------------------|
| Size distribution calculated for $\mu = 0.005$ | 1.0209e-05 | 4.47983e-06 |
| Size distribution grown from $\mu = 0.0008$ | 1.2824e-05 | 4.47983e-06 |

The first results row used a size distribution calculated directly for a median crack size $\mu = 0.005$. The value obtained when the crack size distribution is extended to the critical crack size matches that obtained using a MathCAD calculation. The second results row used an initial crack size distribution for a median crack size $\mu = 0.0008$. This was projected to a time for 3800 hours, corresponding to exponential growth. The final median crack size after the growth projection was $\mu = 0.005$. The difference between the two values in the first results column can be attributed to differences in table interpolation for $F(a_c)$. In the second results column, the same probability of failure was obtained for both rows. In both cases, the value at $F(a_c)$ was extrapolated and accounted for most of the contribution to the probability of failure.

B.4.3 Example 3

Example 3 is the PROF sample problem. A summary of the probability of failure calculation at time 0 is shown in Table B-7:

Table B-7. Example 3: Summary of Results

| | | | |
|--|-------|---------|---------------|
| time = 0 | | | |
| a_critical = 0.5 | | | |
| last tabulated a = 0.045 (F(a) = 0.9999) | | | |
| 1-F(a_critical) extrapolated = 0 | | | |
| F(a) | evals | percent | subtotal |
| 0.99811 | 235 | 29.406 | 4.359658e-011 |
| ----- | | | |
| 1.00000 | 163 | 70.587 | 1.046279e-010 |
| probability of failure = 1.482245e-010 | | | |

The PROF output divides the calculation into two parts, an interpolated region (above the dashed line) and an extrapolated region (below the line). In this example, there is no contribution due to exceeding a_c prior to the flight. The results for other versions of PROF are shown below:

| | |
|---------------|-----------|
| New version | 1.483e-10 |
| WinProf | 4.439e-10 |
| Original PROF | 1.999e-10 |

The results for the original PROF were taken from WL-TR-91-3066 (Volume 1), page 55. This example demonstrates that the changes in calculations did not significantly affect the results obtained for the example problem.

B.5 Inspection and Repair Calculations

At the end of a usage interval, the crack size distribution is modified to reflect maintenance actions. The crack size distribution changes during maintenance because detected cracks are repaired. Repaired details are modeled by a distribution function of equivalent initial crack sizes that reflect the quality of repairs.

The inspection process involves determining the proportion P of cracks that are found during inspection, given by

$$P = \int_0^{\infty} \text{POD}(a) f(a) da \quad (\text{B15})$$

where $\text{POD}(a)$ is the probability of detecting a crack of size a , and $f(a)$ is the crack size density function just prior to maintenance.

We also need intermediate values of this function, namely the probability of finding a crack smaller than a . We define $P(a)$ as

$$P(a) = \int_0^a \text{POD}(a) f(a) da \quad (\text{B16})$$

The calculation of $P(a)$ is actually performed incrementally, using the crack-size distribution function $F(a)$, as

$$P_i(a) = \int_{F_{i-1}}^{F_i} \text{POD}(F^{-1}(u)) du \quad (\text{B17})$$

The integration is done using Simpson's method with a fixed number of panels.

The tabulated distribution function is extrapolated from the last tabulated value F_n using

$$F_e(a) = 1 - \exp(-\lambda(a - \gamma)) \quad (\text{B18})$$

The integral over the extrapolation region

$$P_e(a) = \int_{a_n}^{\infty} \text{POD}(a) f(a) da \quad (\text{B19})$$

is calculated using the Laguerre method.

Repair quality is expressed in terms of the equivalent repair crack size distribution $f_R(a)$.

If $f_{\text{before}}(a)$ and $f_{\text{after}}(a)$ represent the density function of crack sizes in the population of structural details before and after a maintenance action, then

$$f_{\text{after}}(a) = P \cdot f_R(a) + [1 - \text{POD}(a)] \cdot f_{\text{before}}(a) \quad (\text{B20})$$

where P is the fractional proportion of cracks that will be detected by the inspection. The post maintenance crack size is then projected forward for the next interval of uninspected usage.

B.6 Procedure for Inspection and Repair Calculations

The cumulative distribution function of the crack size after repair is given by:

$$F_{\text{after}}(a) = P \cdot F_R(a) + F_{\text{before}}(a) - P(a) \quad (\text{B21})$$

where

$$P(a) = \int_0^a \text{POD}(a) f_{\text{before}}(a) da \quad (\text{B22})$$

Calculation of $F_{\text{after}}(a)$ proceeds as follows:

1. Construct a table that contains all the crack sizes in both the current crack size distribution and the equivalent repair crack size distribution tables.
2. For each point in the current crack size distribution, calculate

$$F^*(a_i) = F_{\text{before}}(a_i) - P(a_i) \quad (\text{B23})$$

where $P(a_i)$ is calculated incrementally as

$$P(a_i) = P_i(a) + P(a_{i-1}) \quad (\text{B24})$$

3. For each point in the combined table of crack sizes, calculate

$$F_{\text{after}}(a_i) = P \cdot F_R(a_i) + F^*(a_i) \quad (\text{B25})$$

4. At this point the cumulative probabilities of $F_{\text{after}}(a)$ do not correspond to those in the original crack-size distribution table. Interpolate the inverse table to calculate crack sizes corresponding to the original crack-size distribution values.